Il segnale Chirp ed
i codici a fase quadratica

Pierfrancesco Lombardo

CHIRP: linear frequency modulated signal

MAXIMUM RADAR RANGE

$$R_{max} = \sqrt[4]{\frac{E_T G^2 \lambda^2 \sigma}{(4\pi)^3 K T_0 F S_a}}$$

Con $E_T = P_p T$

RANGE RESOLUTION

$$R_d = \frac{cT}{2}$$

CHIRP: LINEAR FREQUENCY MODULATION

$$s(t) = e^{j2\pi\left(f_p t + \frac{B}{T}\cdot\frac{t^2}{2}\right)} \mathrm{rect}_T(t)$$

B chirp bandwidth
T transmitted pulse length
f_p (residual) carrier frequency

- CHIRP (long pulse with phase coding): has the power properties of the long pulse and the resolution properties of the short pulse.

- Phase coding → waveform compression by means of matched filtering

CHIRP: Time domain waveform (I)

$$s(t) = e^{j2\pi(f_p t + \frac{B}{T}\cdot\frac{t^2}{2})}\,\mathrm{rect}_T(t)$$

- CHIRP MODULUS DEL |s(t)|:

$$|s(t)| = \begin{cases} 1 & \text{Per } |t| \le T/2 \\ 0 & \text{Per } |t| \ge T/2 \end{cases}$$

- CHIRP PHASE Φ(t)

$$\Phi(t) = 2\pi(f_p t + \frac{B}{T}\cdot\frac{t^2}{2})$$

- INSTANTANEOUS FREQUENCY f(t)

$$f(t) = \frac{1}{2\pi}\cdot\frac{d\Phi(t)}{dt} = f_p + \frac{B}{T}t$$

$f(-T/2)=f_p-B/2$

$f(T/2)=f_p+B/2$

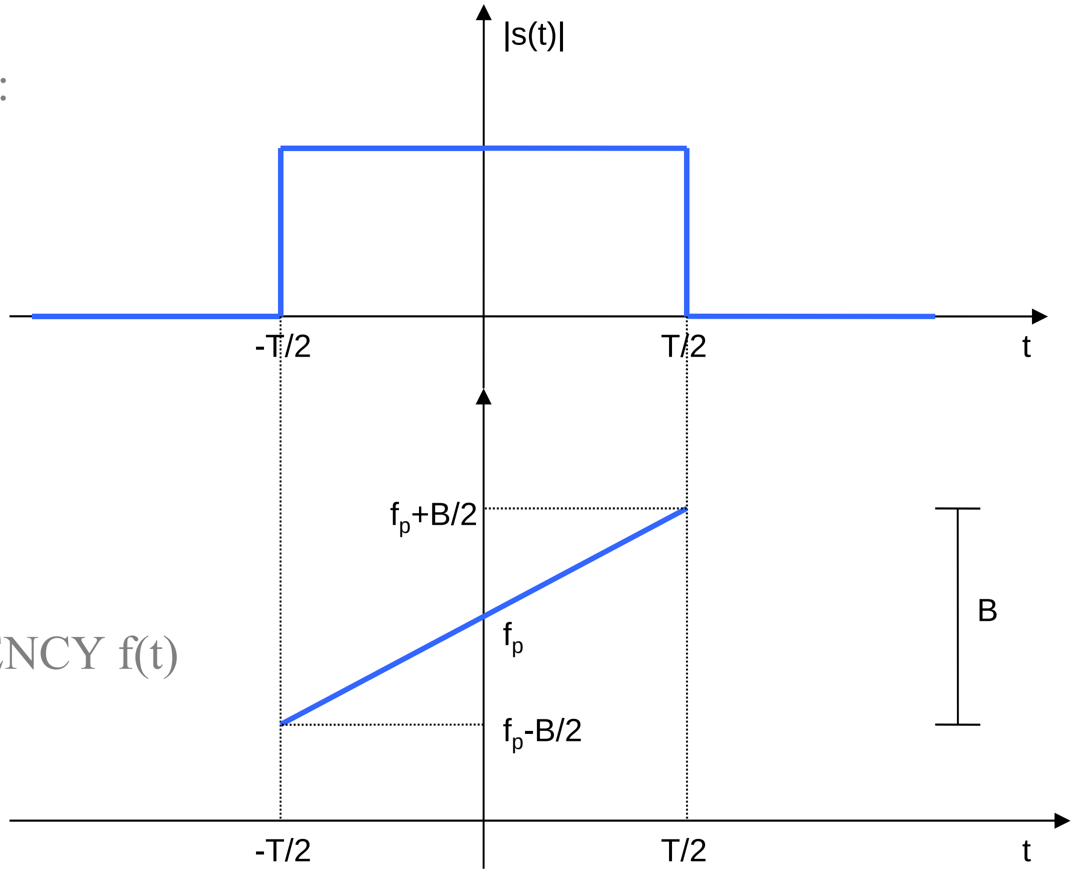

Frequency modulation

CHIRP: Time domain waveform (II)

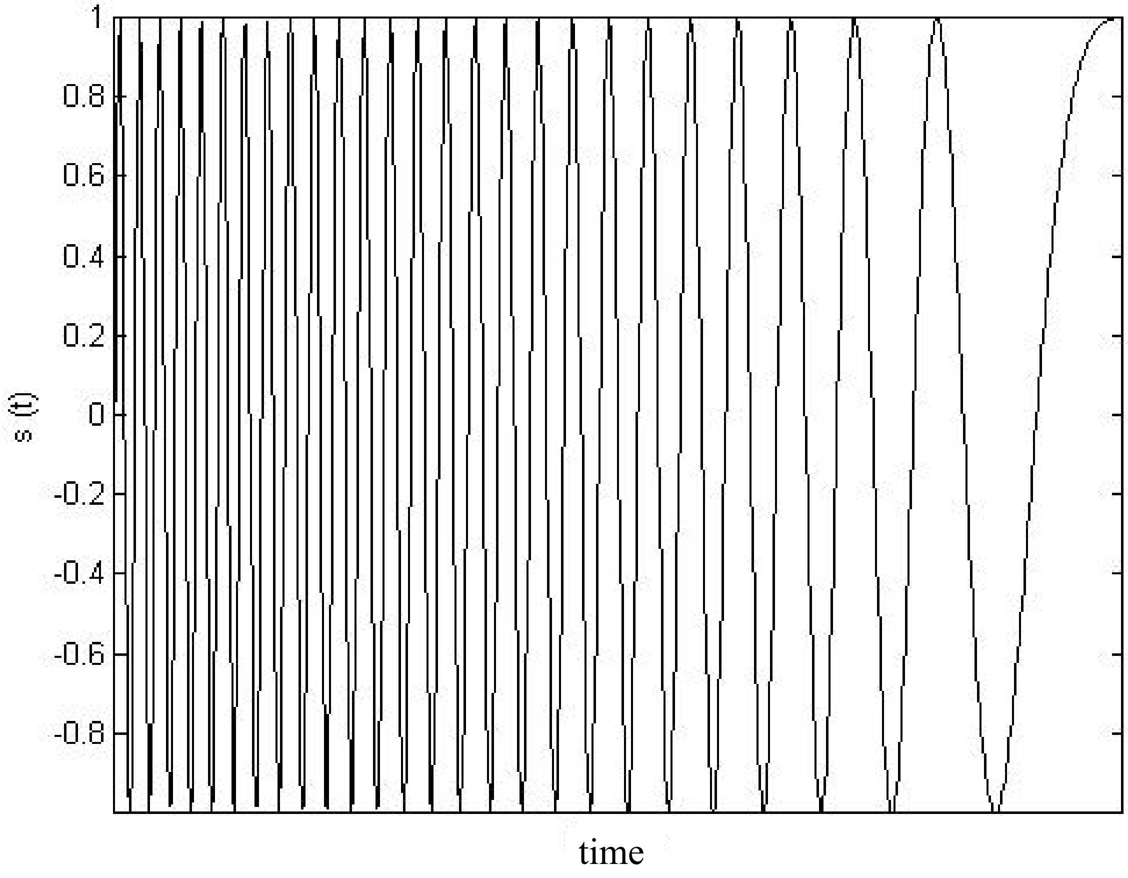

CHIRP: Time domain waveform (III)

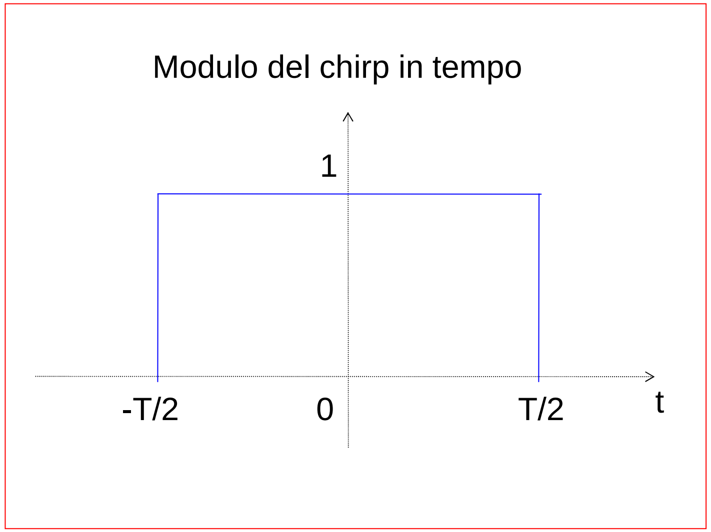

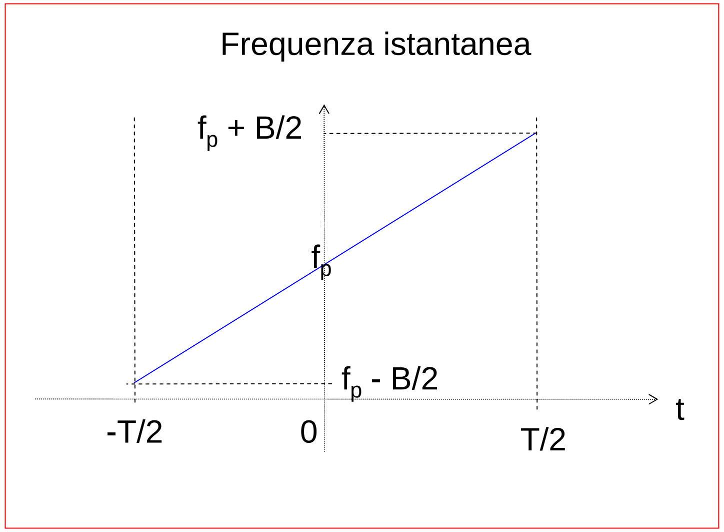

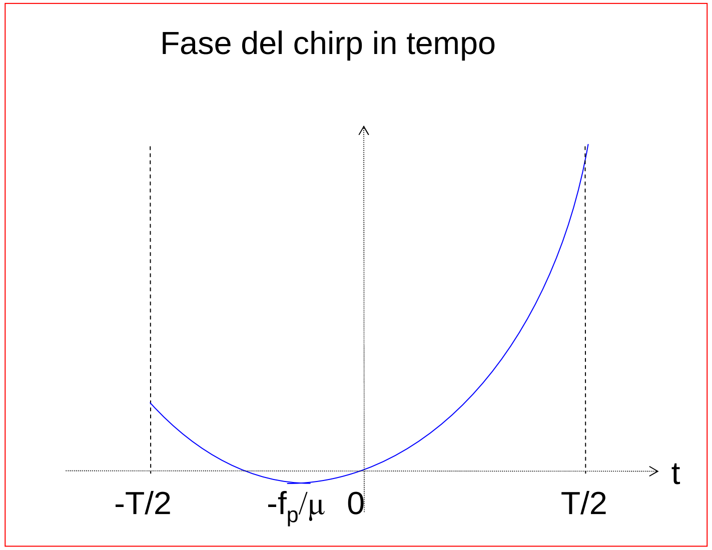

Sistemi Radar

CHIRP: Frequency domain waveform (I)

Fourier Transform of the chirp signal:

$$S(f)=\frac{1}{\sqrt{2\mu}}\{[C(X_1)+C(X_2)]+j[S(X_1)+S(X_2)]\}e^{-j\frac{\pi}{\mu}f^2}=|S(f)|e^{j\Phi(f)}$$

C(X) Fresnel cosine
S(X) Fresnel sine

$$X_1=\sqrt{2BT}\left(\frac{1}{2}+\frac{f}{B}\right)$$

$$X_2=\sqrt{2BT}\left(\frac{1}{2}-\frac{f}{B}\right)$$

- ✓ The compression factor BT determines the frequency domain characteristics of the chirp waveform

AMPLITUDE SPECTRUM

$$|S(f)|=\frac{1}{\sqrt{2\mu}}\sqrt{[C(X_1)+C(X_2)]^2+[S(X_1)+S(X_2)]^2}$$

For high BT values (BT>100)

$$|S(f)|\cong\frac{1}{\sqrt{2\mu}}\sqrt{2}=\frac{1}{\sqrt{\mu}}=\sqrt{\frac{T}{B}}\qquad |f|\le B/2$$

PHASE SPECTRUM

$$\Phi(f)=-\frac{\pi}{\mu}f^2+\mathrm{atg}\left[\frac{S(X_1)+S(X_2)}{C(X_1)+C(X_2)}\right]$$

For high BT values (BT>100)

$$\Phi(f)\cong-\frac{\pi}{\mu}f^2+\frac{\pi}{4}\qquad |f|\le B/2$$

$$S(f)=\sqrt{\frac{T}{B}}e^{-j\left[\pi\frac{T}{B}f^2-\frac{\pi}{4}\right]}\mathrm{rect}_B(f)$$

Funzioni Coseno e Seno Integrale

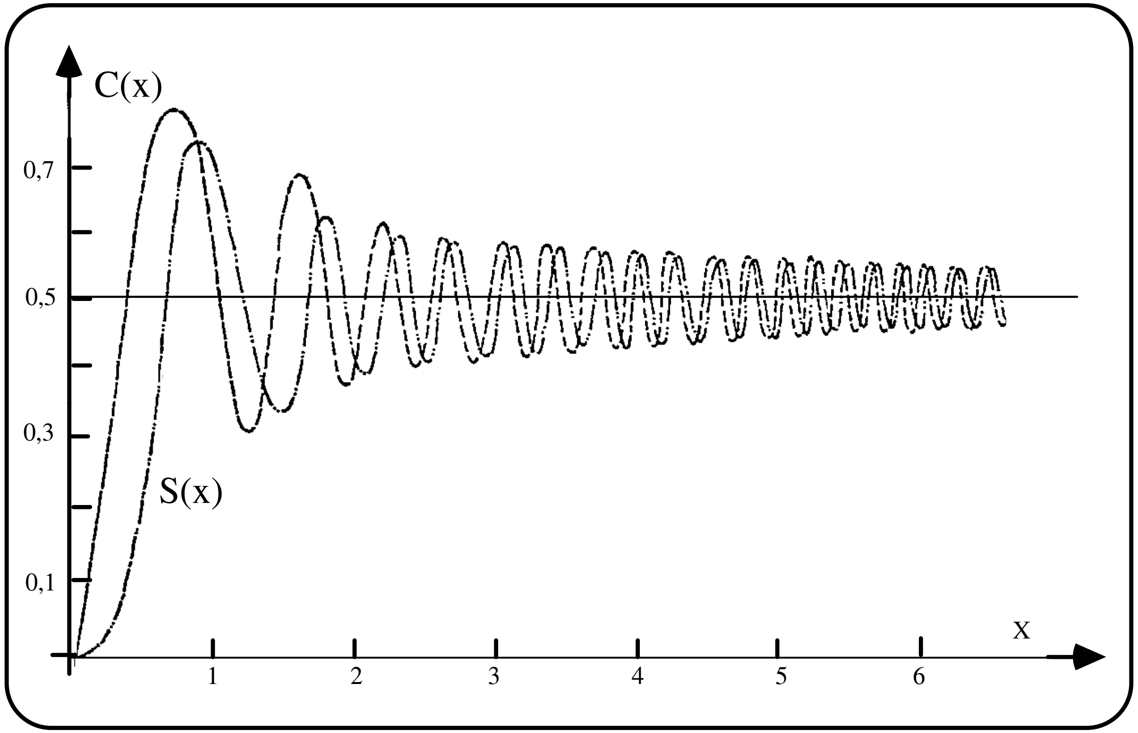

CHIRP: Frequency domain waveform (II)

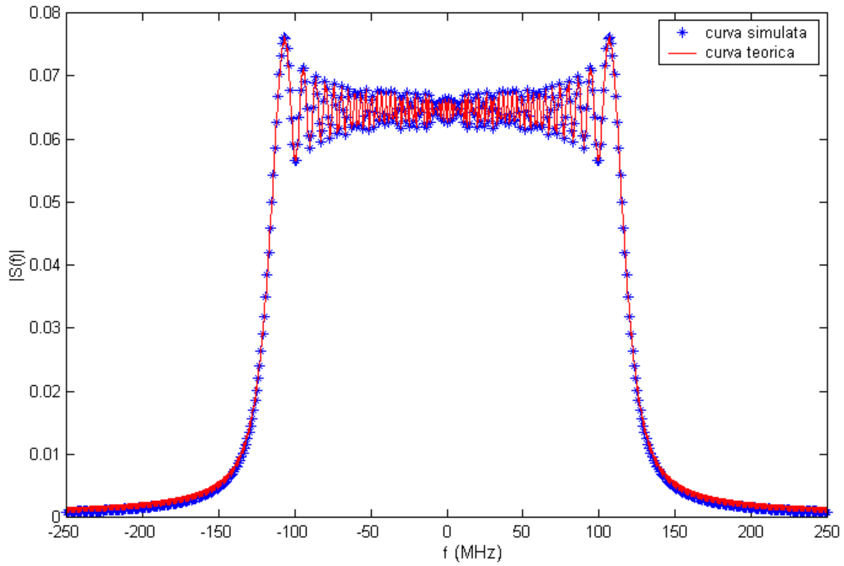

Chirp amplitude spectrum for B=240MHz, T=1µs

Chirp phase spectrum for B=240MHz, T=1µs

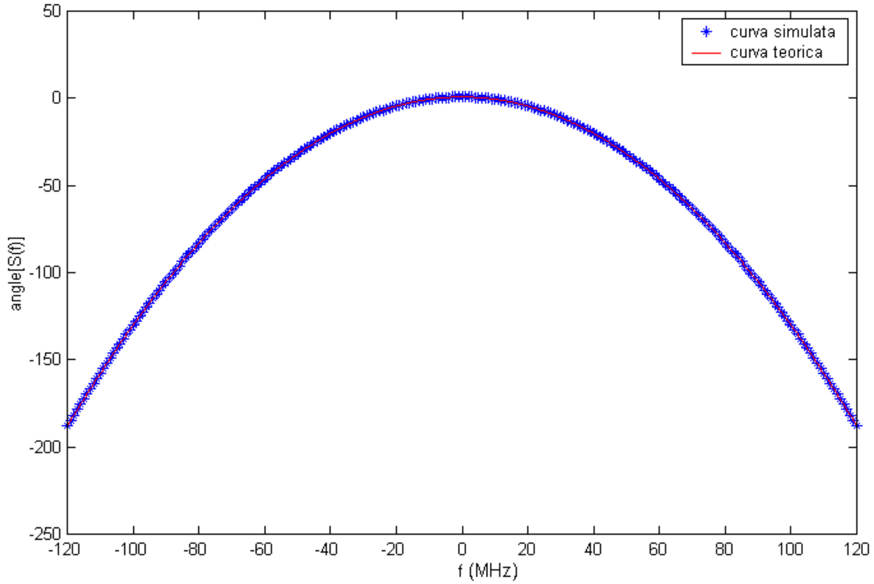

CHIRP: Frequency domain waveform (III)

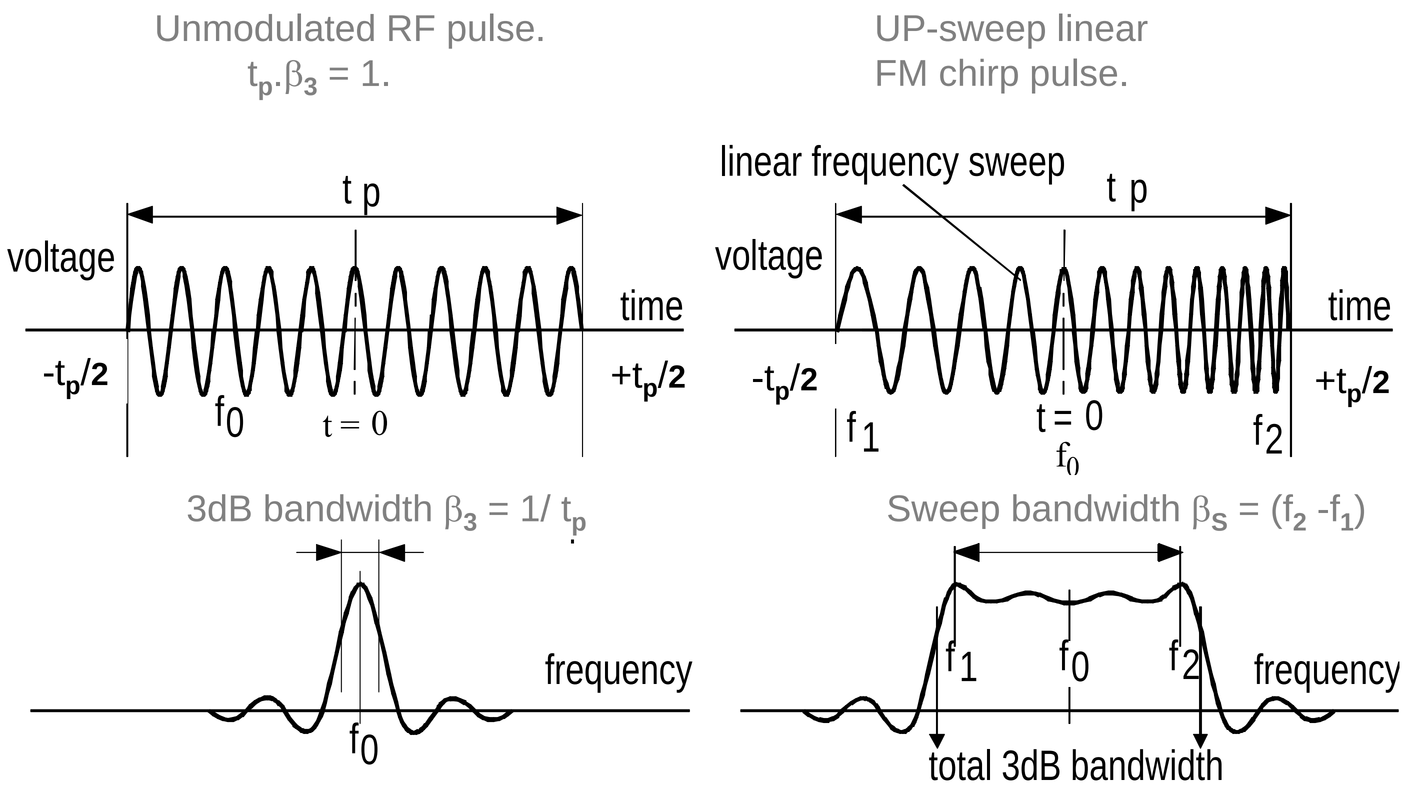

Autocorrelazione del chirp (I)

Funzione di Ambiguità: Chirp con inviluppo rettangolare

$$s_0(t) = \frac{1}{\sqrt{\tau_p}} rect_{\tau_p}(t)\ e^{j\pi k t^2}$$

$$|\chi(\tau,0)| = \left| (1-\frac{|\tau|}{\tau_p}) \sin c[\pi k \tau \tau_p (1-\frac{|\tau|}{\tau_p})] \right|, \qquad |\tau| \le \tau_p$$

Primo nullo

$$\pi k \tau \tau_p (1-\frac{|\tau|}{\tau_p}) = \pi$$

$$\tau \tau_p - \tau^2 = \frac{1}{k}$$

$$\tau^2 - \tau \tau_p + \frac{1}{k} = 0$$

$$\tau = \frac{\tau_p}{2} - \sqrt{\frac{\tau_p^2}{4} - \frac{1}{k}} =$$

$$= \frac{\tau_p}{2} - \frac{\tau_p}{2}\sqrt{1-\frac{4}{k\tau_p^2}} =$$

$$\approx \frac{\tau_p}{2} - \frac{\tau_p}{2}\left(1-\frac{2}{k\tau_p^2}\right) = \frac{1}{k\tau_p} = \frac{1}{B_p}$$

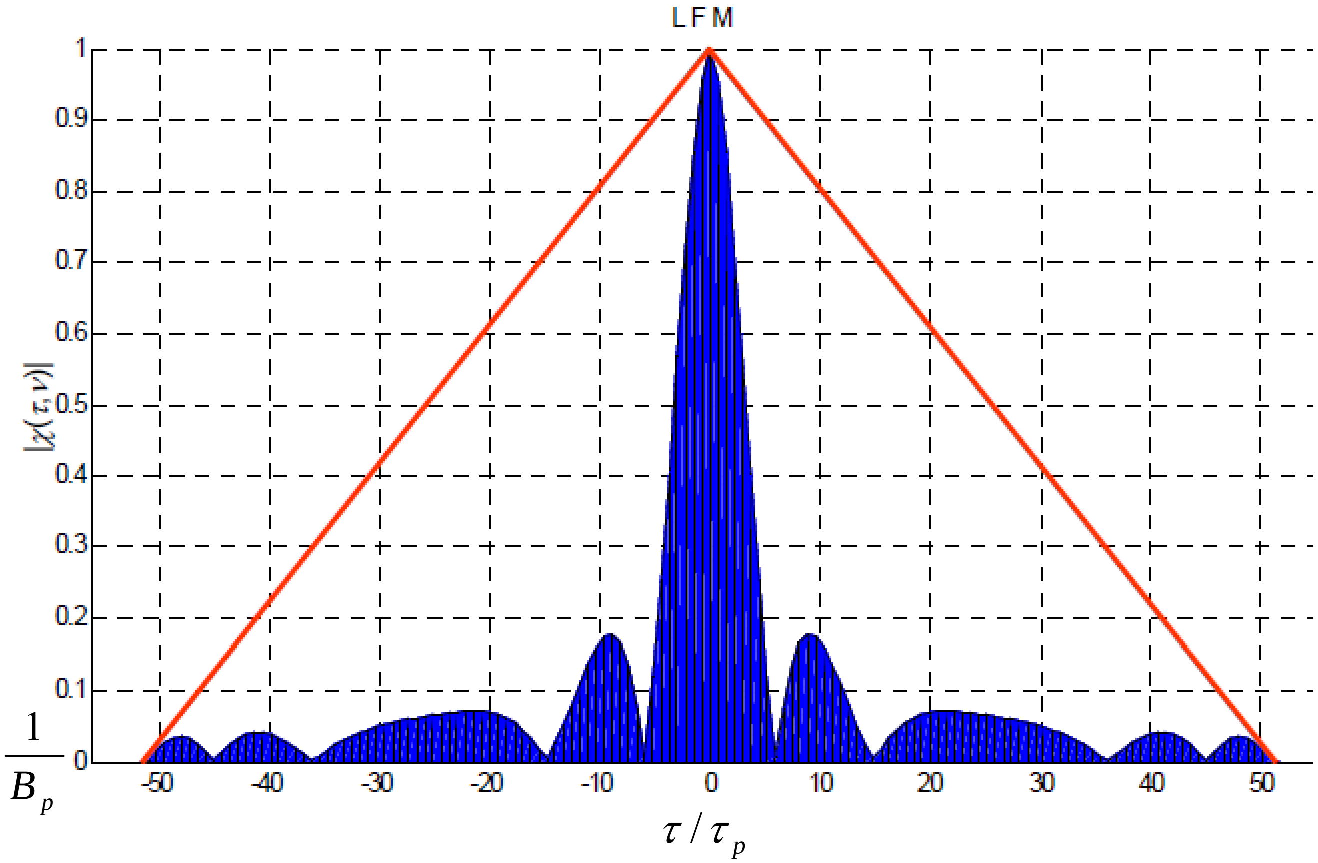

Funzione di autocorrelazione del chirp (III)

Funzione di Ambiguità: Chirp con inviluppo rettangolare

$$s_0(t) = \frac{1}{\sqrt{\tau_p}} rect_{\tau_p}(t)\ e^{j\pi k t^2}$$

$$\left|\chi(\tau,0)\right| = \left| \ (1-\frac{|\tau|}{\tau_p})\sin c[\pi k \tau \tau_p (1-\frac{|\tau|}{\tau_p})] \right| , \qquad |\tau| \le \tau_p$$

Rapporto di compressione

$$\frac{\tau_p}{\frac{1}{k\tau_p}} = k\ \tau_p^2 = B_p\ \tau_p$$

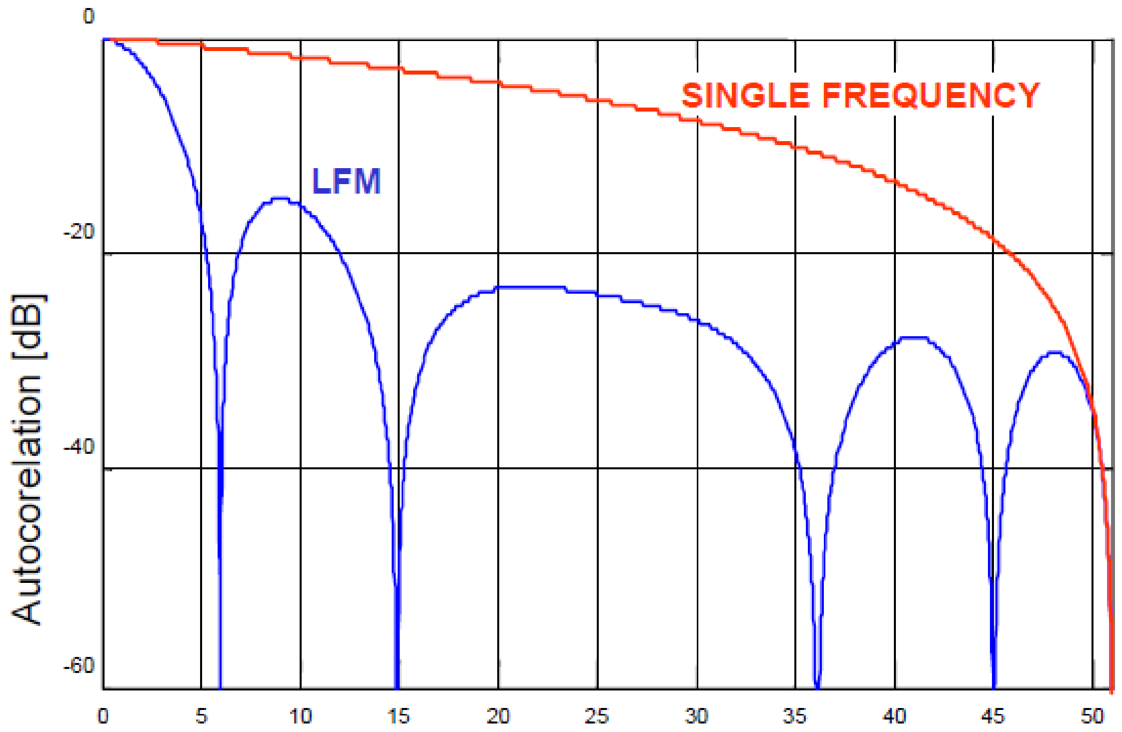

τ / τ_p

Chirp approximation and sidelobes (I)

- Chirp autocorrelation (matched filter output)

$$g(t) = \sqrt{\frac{B}{T}} \frac{\sin\left[\pi \frac{B}{T}\left(T - |t|\right)t\right]}{\pi \frac{B}{T} t}$$

- approximated with

$$g(t) \cong \sqrt{\frac{B}{T}} \frac{\sin\left[\pi B t\right]}{\pi \frac{B}{T} t} = \sqrt{BT} \quad \sin c\left[\pi\, B\, t\right]$$

which is the Inverse Fourier Transform of a rectangle in the frequency domain

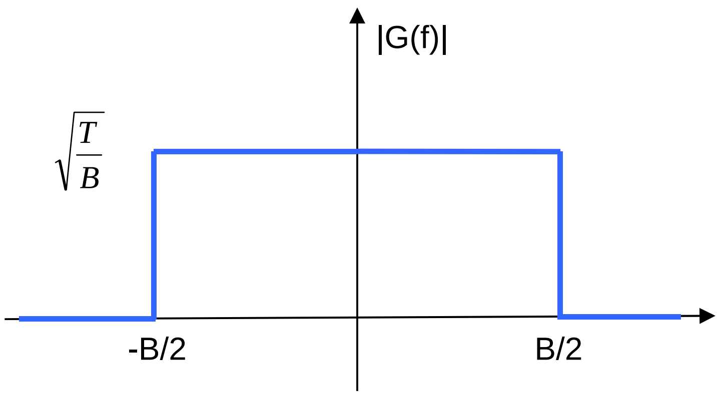

$$G(f) = \sqrt{\frac{T}{B}} \; rect_B(f)$$

Pulse compression technique (I)

- **Matched Filter**

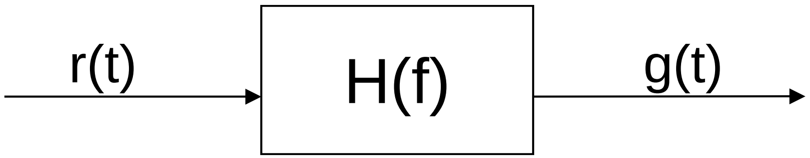

$$r(t) = e^{j2\pi\left(f_p t + \frac{B}{T}\cdot\frac{t^2}{2}\right)} \mathrm{rect}_T(t)$$ Received signal

$$h(t) = \sqrt{\frac{B}{T}} e^{-j2\pi\left(-f_p t + \frac{B}{T}\cdot\frac{t^2}{2}\right)} \mathrm{rect}_T(t)$$ matched filter impulse response

$$g(t) = r(t) * h(t) = \int_{-\infty}^{\infty} r(\tau)h(t-\tau)d\tau$$ matched filter output

$$g(t) = \sqrt{\frac{B}{T}} \frac{\mathrm{sen}\left[\pi \frac{B}{T}(T - |t|)t\right]}{\pi \frac{B}{T} t} \cdot e^{j2\pi f_p t}$$

sin x/x signal envelope: with -4dB aperture =1/B.

✓ g(t) autocorrelation of the input signal (f_d=0).
✓ for $f_d \neq 0$ mismatched filter

The pulse has been compressed to: $\tau_c = 1/B < T$

Pulse compression technique (II)

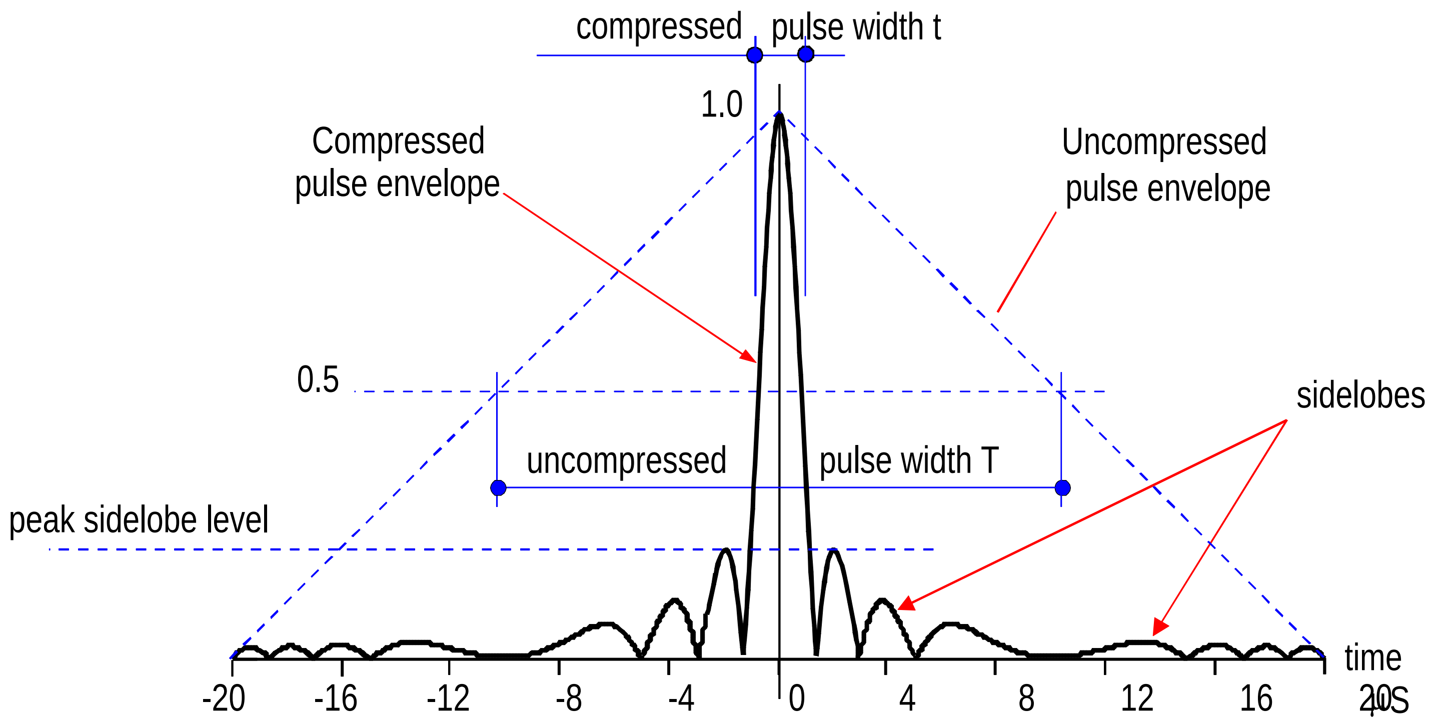

The width of the main lobe of the compressed pulse is $1/\beta_s$ ie. $\frac{1}{\text{sweep bandwidth}}$

Pulse compression technique (III)

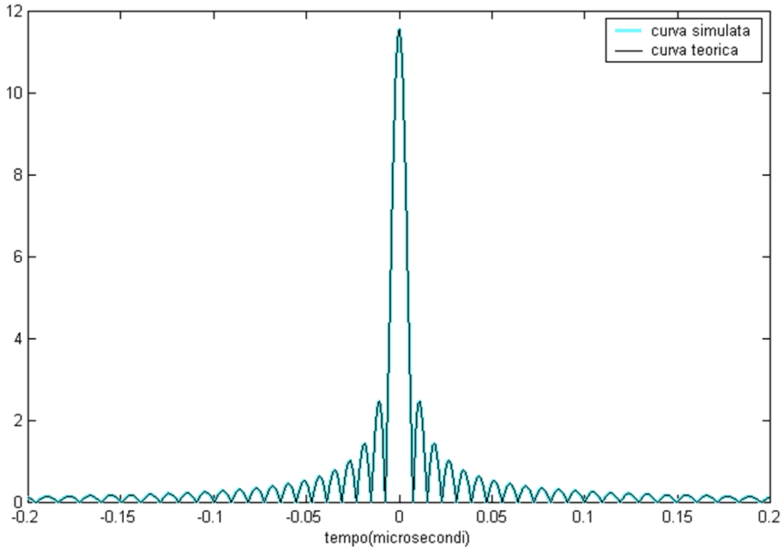

Matched filter output

Matched filter output
for: B=133.5 MHz
and T=1 μs

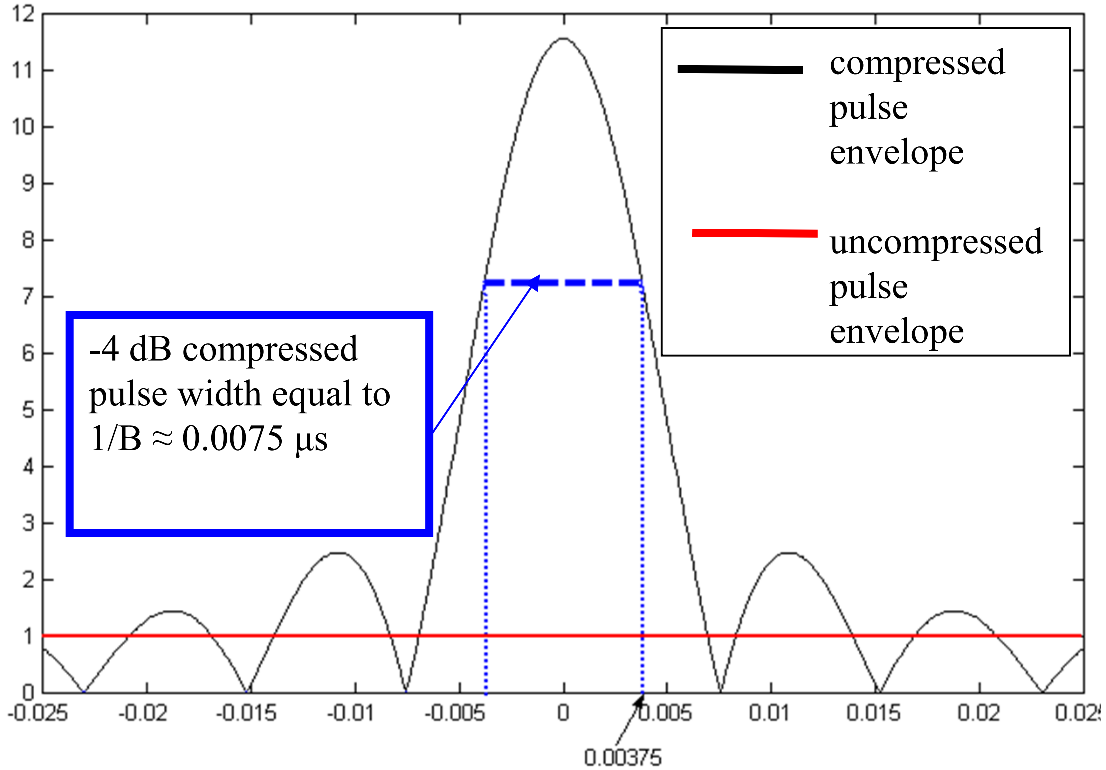

Pulse compression technique (IV)

Matched filter output : sidelobes

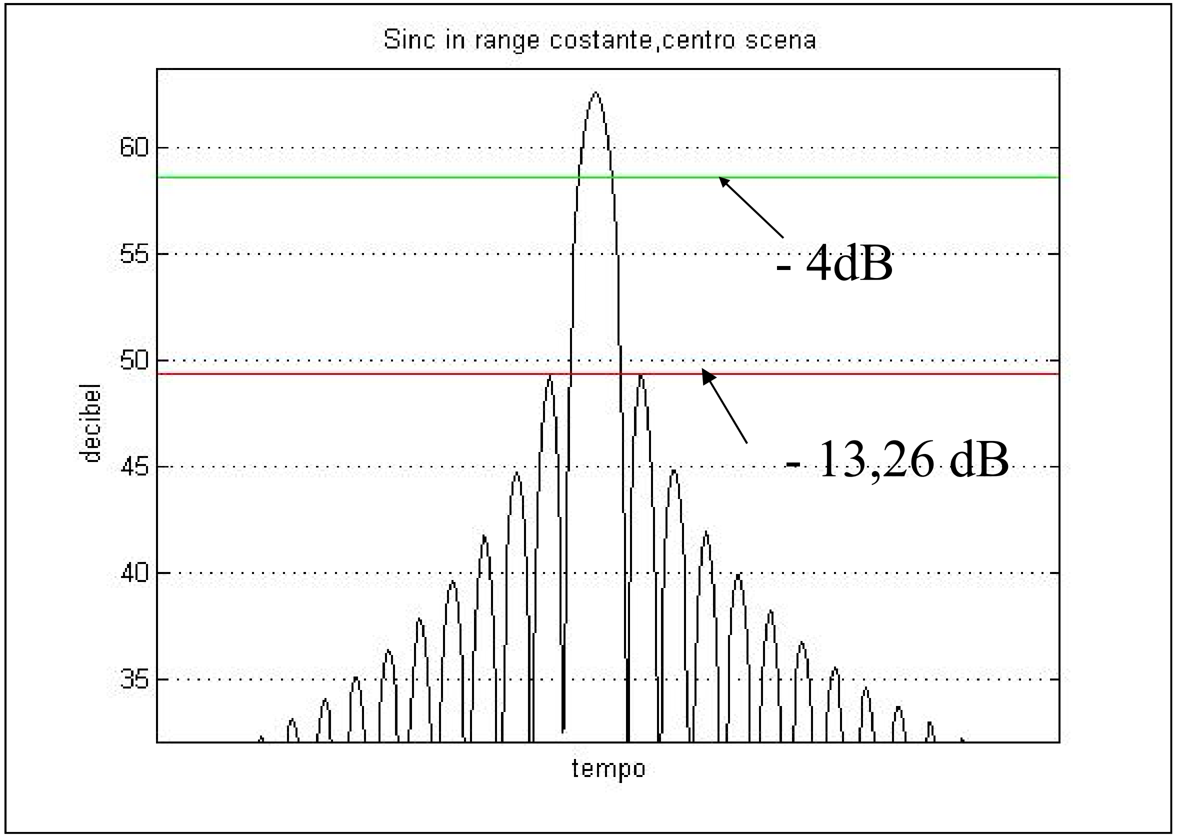

SAW pulse compression (I)

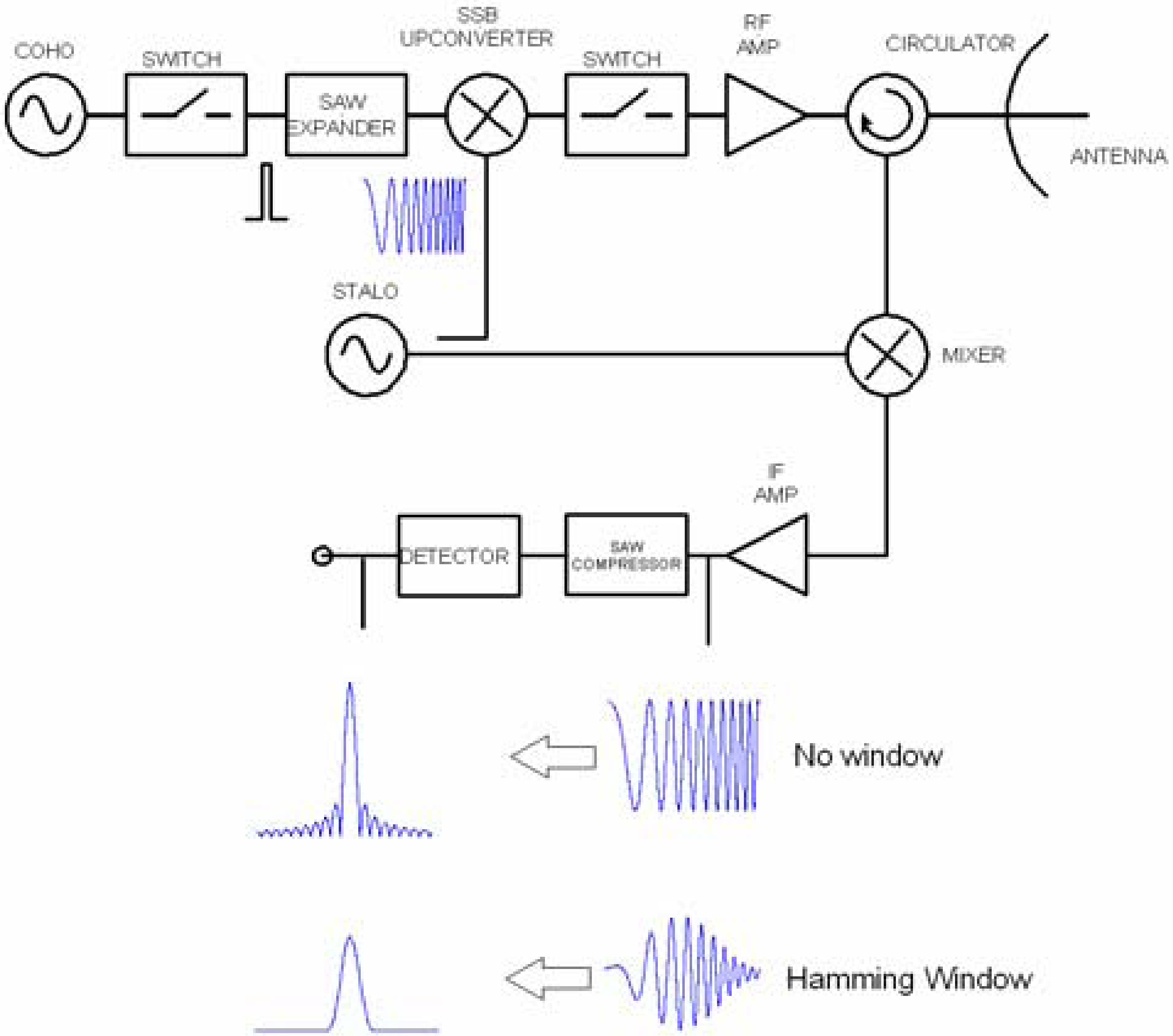

SAW pulse compression (II)

- In a pulse compression system, a very brief pulse consisting of a range of frequencies passes through a dispersive delay line (SAW expander) in which its components are delayed in proportion to their frequency.
- In the process the pulse is stretched; for example a 1ns pulse may be lengthened by a factor of 1000 to a duration of 1μs before it is up-converted amplified and transmitted.
- A constant amplitude waveform is produced in which the frequency increases or decreases linearly by Δf over the duration of the pulse

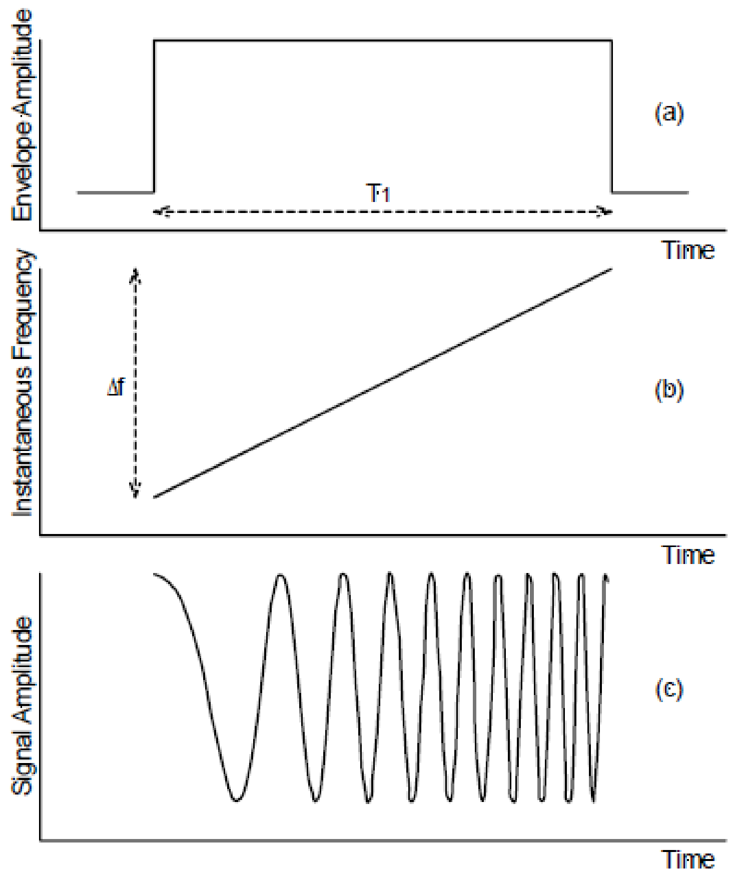

SAW pulse compression (III)

- The echo returns from the target are down converted and amplified
- It is then passed through a pulse compression filter which is designed so that the velocity of propagation is proportional to frequency
- The pulse is compressed to a width $1/\Delta f$
- The compressed echo yields nearly all of the information that would have been available had the unaltered 1ns pulse been transmitted.
- The amount of signal-to-noise ratio (SNR) gain achieved is approximately equivalent to the pulse time-bandwidth product $\beta.\tau$.
- Most pulse compression systems use surface acoustic wave (SAW) technology to implement the pulse expansion and compression functions
- The maximum $\beta.\tau$ product that is readily available is about 1000.

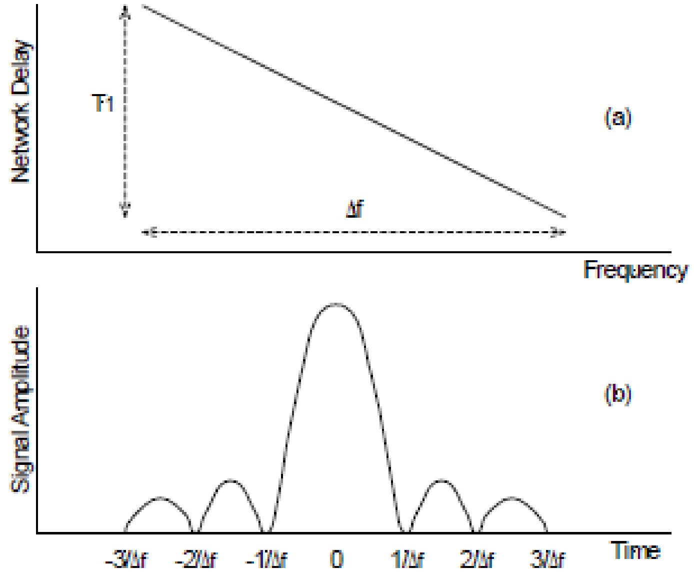

SAW pulse compression (IV)

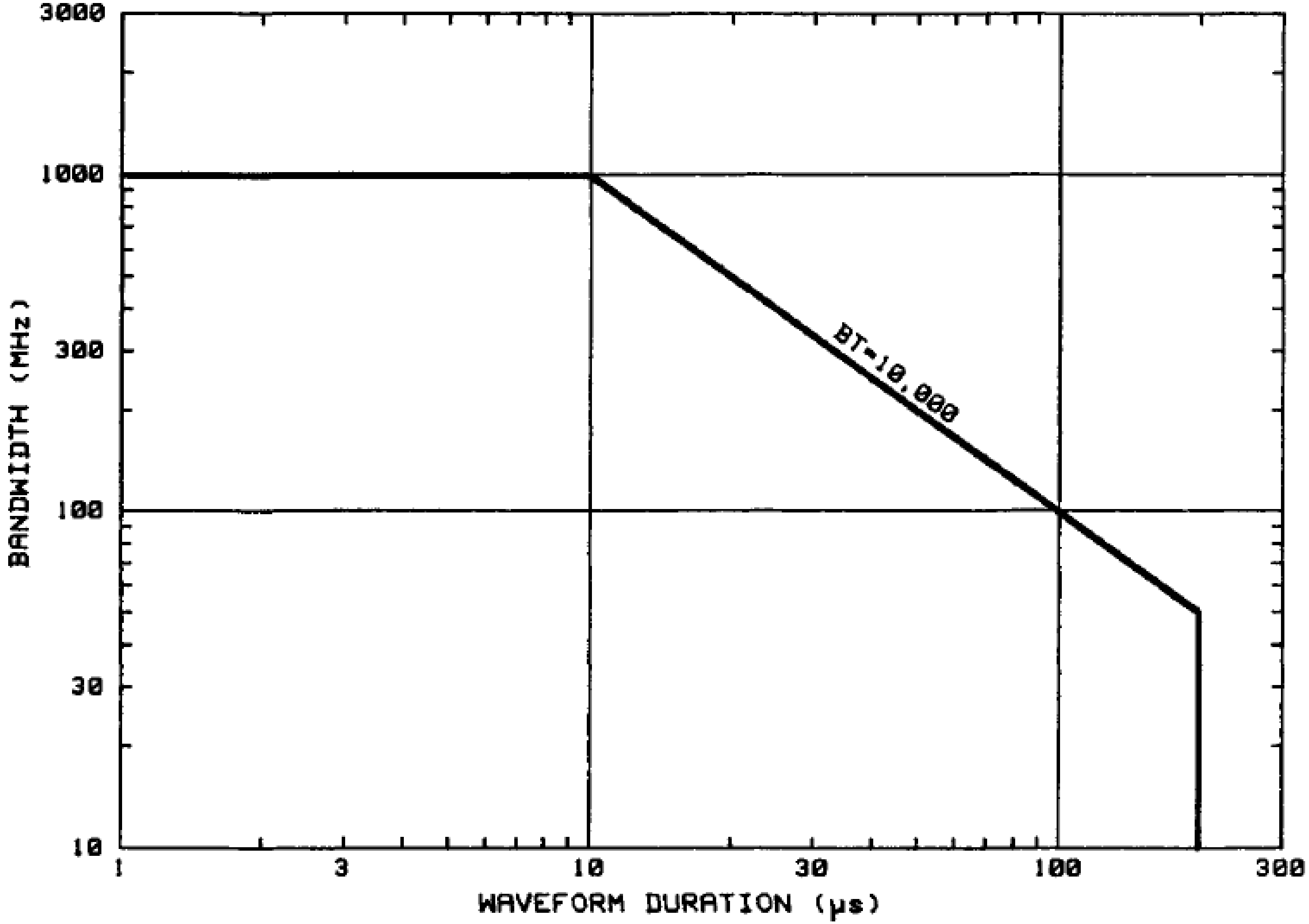

Chirp approximation and sidelobes

- Chirp autocorrelation (matched filter output)

$$g(t) = \sqrt{\frac{B}{T}} \frac{\sin\left[\pi \frac{B}{T}\left(T - |t|\right)t\right]}{\pi \frac{B}{T} t}$$

- approximated with

$$g(t) \cong \sqrt{\frac{B}{T}} \frac{\sin[\pi B t]}{\pi \frac{B}{T} t} = \sqrt{BT} \ \sin c\ [\pi\, B\, t]$$

which is the Inverse Fourier Transform of a rectangle in the frequency domain

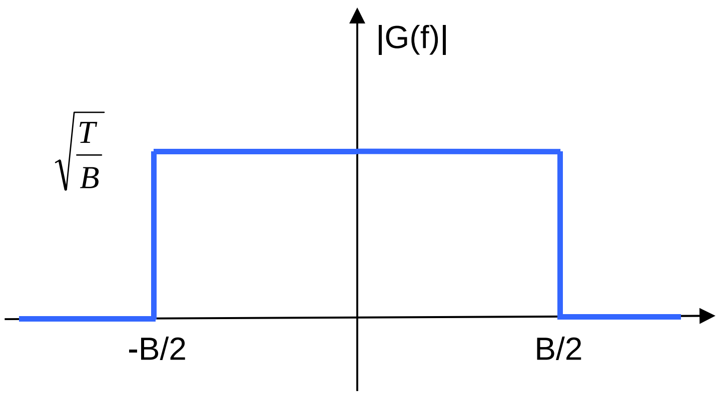

$$G(f) = \sqrt{\frac{T}{B}} \ rect_B(f)$$

Frequency domain weighting (I)

- To control sidelobes of the compressed waveform, amplitude weighting with appropriate tape functions can be used

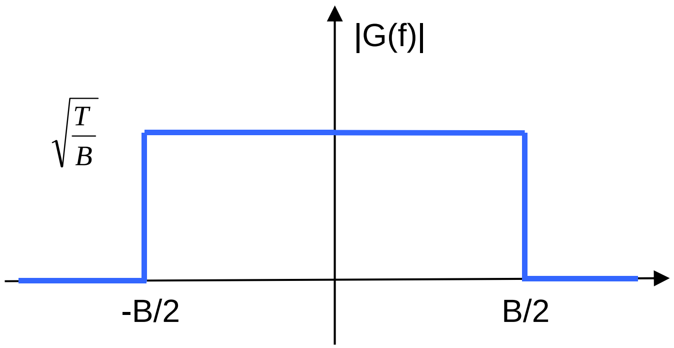

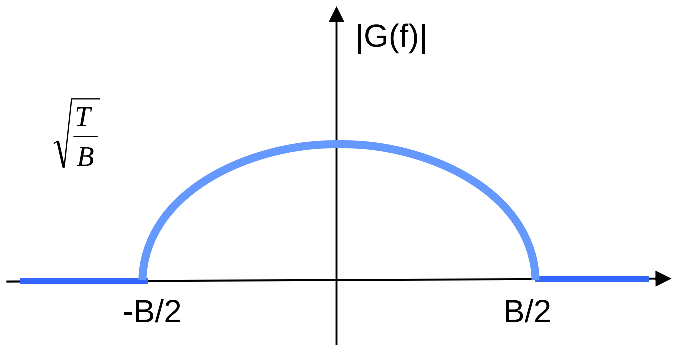

$$G(f)=\sqrt{\frac{T}{B}}\ rect_B(f) \quad \Rightarrow \quad G(f)=\sqrt{\frac{T}{B}}\ rect_B(f)\ \cdot\ W(f)$$

Taking the Inverse Fourier Transform, we have in time domain

$$g(t) \cong \sqrt{BT}\ \ \text{sinc}\ [\pi B t] \quad \Rightarrow \quad g(t) \cong \sqrt{BT}\ \ \text{sinc}\ [\pi B t] * w(t)$$

Frequency domain weighting (II)

- using appropriate taper function, allows to control sidelobes

For example

$$W(f) = (1-k) + k\ \cos(\pi \frac{f}{B})$$

$$w(t) = (1-k)\ \delta(t) + \frac{k}{2}\ \delta(t - \frac{1}{2B}) + \frac{k}{2}\ \delta(t + \frac{1}{2B})$$

Shifted replicas to remove sidelobes …

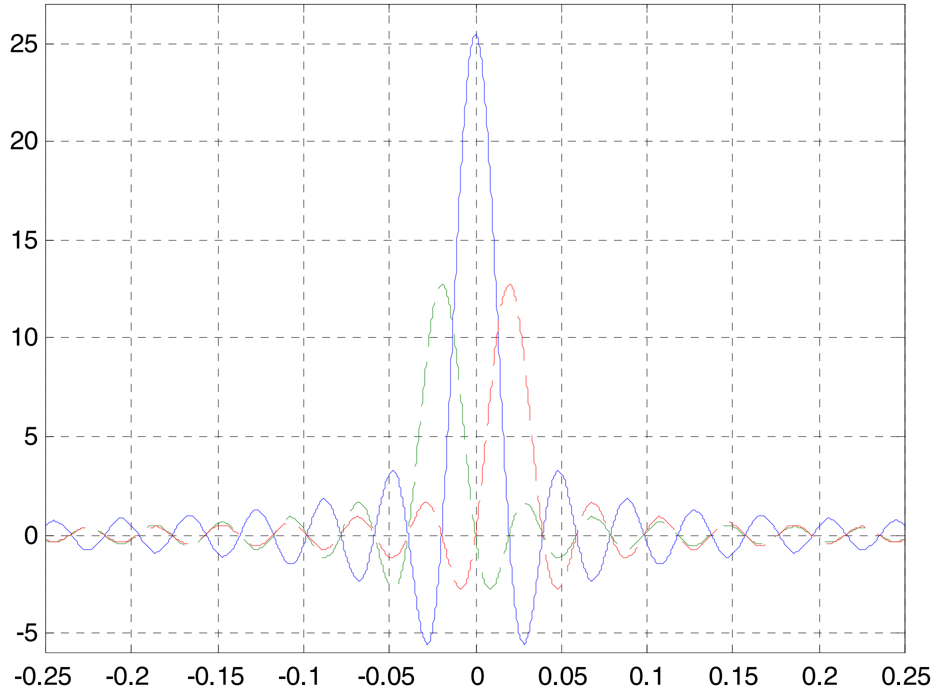

$$g(t) \cong \sqrt{BT}\ \left\{ (1-k)\ \text{sinc}\ [\pi B t] + \frac{k}{2}\ \text{sinc}\left[\pi B (t - \frac{1}{2B})\right] + \frac{k}{2}\ \text{sinc}\left[\pi B (t - \frac{1}{2B})\right] \right\}$$

Analog vs. Digital domain operations

- usually compression is applied in the sampled domain
- Starting from an approximately rectangular chirp spectrum (sampled in frequency at 1/T)

$$g(t_n) = \sum_{k=-\frac{(N-1)}{2}}^{\frac{(N-1)}{2}} e^{+j\frac{2\pi}{T}k\,t_n} = \frac{\sin\left[\frac{\pi}{T}(N-1)t_n\right]}{\sin\left[\frac{\pi}{T}t_n\right]}$$

Zeros of NUM: $t_n = \frac{kT}{N-1}$

Zeros of DEN: $t_n = kT$

which is the Inverse Fourier Transform of a rectangle in the frequency domain

$$g(t_n) = \sum_{k=-\frac{(N-1)}{2}}^{\frac{(N-1)}{2}} w_k\, e^{+j\frac{2\pi}{T}k\,t_n}$$

with $w_k = W(\frac{k}{T})$

Compressed waveform quality parameters

- **Side Lobe Level**

  $$SLL = \frac{\text{Amplitude of the highest Side Lobe}}{\text{Main Beam Peak}}$$

  Side Lobe Ratio

  $SLR=(SLL)^{-1}$

$w_k \rightarrow$ taper coefficients

Generally achieved at the expense of:

- **Efficiency**

$$\eta = \frac{\left(\sum_{k=0}^{N-1} w_k\right)^2}{N\sum_{k=0}^{N-1} w_k^2}$$

- **3 dB resolution**

Taylor (1953):

- Symmetric weights yield lower sidelobes
- The sidelobe decay depends on the discontinuity in the aperture distribution and in its derivatives.
- A weight distribution with non-zero external elements (pedestal) is more efficient

Common used taper functions

	Efficiency η	PSL (dB)	Main lobe width (w.r.t) 1/B.
Uniform	1	-13.3	0.89
Cosine	0.81	-23	1.19
Cosine squared (Hanning)	0.67	-32	1.44
Cosine squared on 10 dB pedestal	0.88	-26	1.08
Cosine squared on 20 dB pedestal	0.75	-40	1.28
Hamming	0.73	-43	1.30
Dolph Chebyshev	0.72	-50	1.33
Dolph Chebyshev	0.66	-60	1.44
Taylor n-bar=3	0.9	-26	1.05
Taylor n-bar=5	0.8	-36	1.18
Taylor n-bar=8	0.73	-46	1.30

Triangle (Bartlett) Window

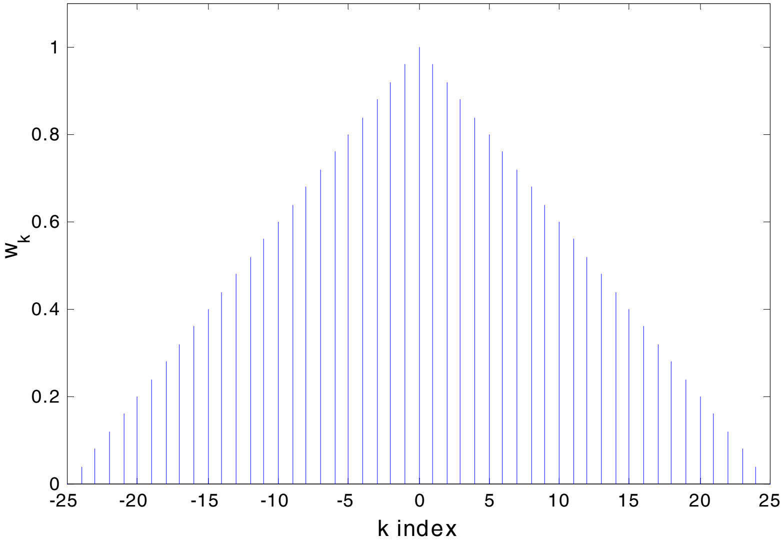

$$w_k = 1 - \frac{|k|}{(N-1)/2} \qquad k = -\frac{N-1}{2},..,-1,0,1,..,\frac{N-1}{2}$$

$$g(t_n) = \frac{2}{N}\left[\frac{\sin\left[\frac{\pi}{T}\frac{N}{2}t_n\right]}{\sin\left[\frac{\pi}{T}t_n\right]}\right]^2$$

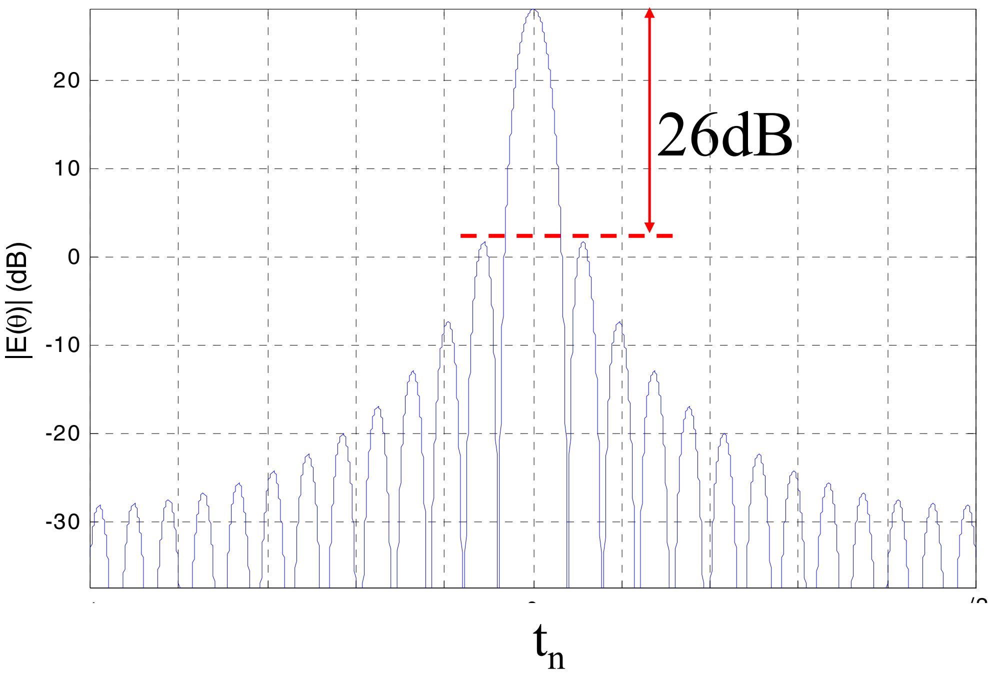

- Main Beam width (between zero crossing) is twice that of the uniform window
- Zeros of order 2 in the Fourier Transform
- SLR≅26dB=2*13dB
- Decay SL ∝ $1/x^2$ (-12dB/oct) (discontinuity in the first derivative)

$\cos^{\alpha}(x)$ Windows

$$w_k = \cos^{\alpha}\left[\frac{k}{N-1}\pi\right] \qquad k = -\frac{N-1}{2},..,-1,0,1,..,\frac{N-1}{2}$$

As α increases, the windows become smoother and the pattern shows increased SLR and faster falloff of the SL, but with an increase width of the ML.

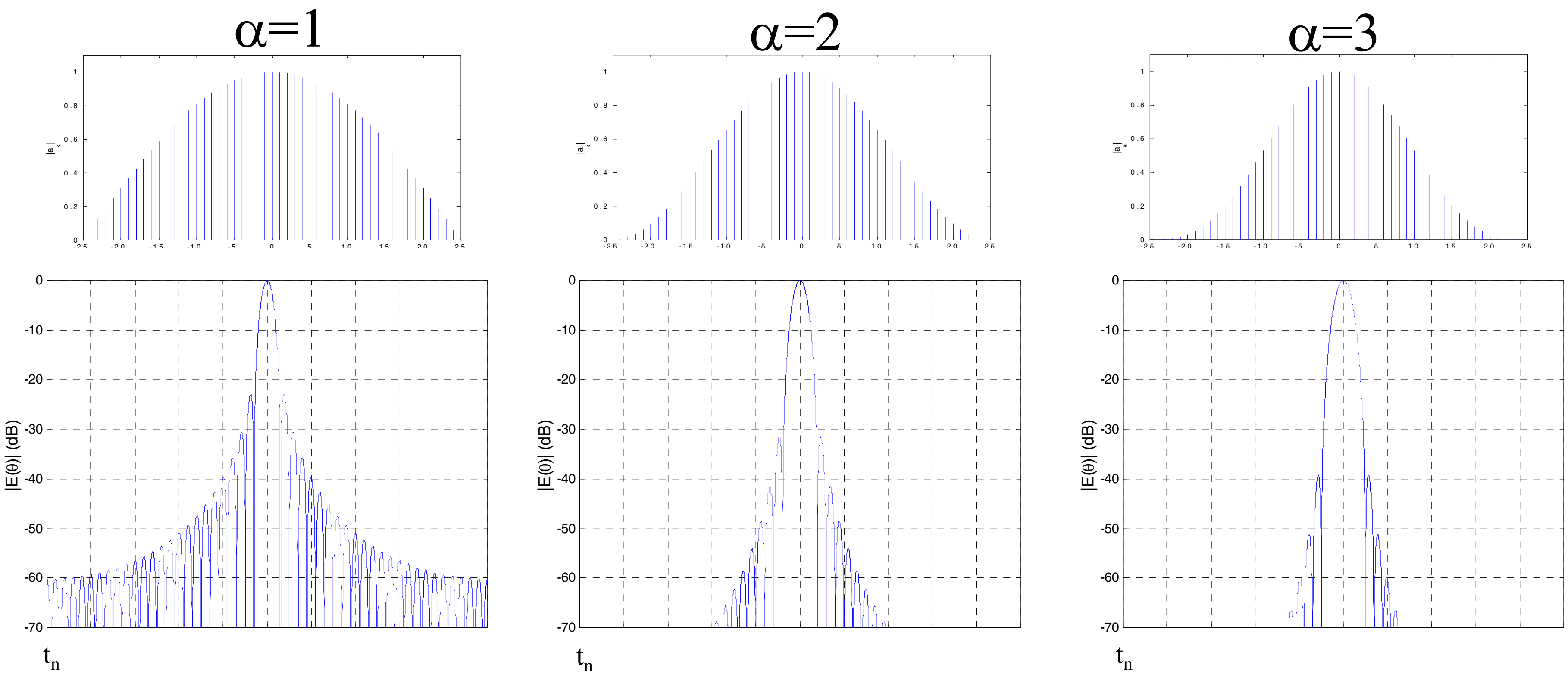

$\cos^{\alpha}(x)$ Windows → Hanning Window (α=2)

$$w_k = \cos^2\left[\frac{k}{N-1}\pi\right] = \frac{1}{2}\left[1+\cos\left[\frac{2k}{N-1}\pi\right]\right] = \frac{1}{2}+\frac{1}{2}\cos\left[\frac{2k}{N-1}\pi\right] \qquad k = -\frac{N-1}{2},..,-1,0,1,..,\frac{N-1}{2}$$

$$g(t_n) = \left\{\frac{1}{2}D(x) + \frac{1}{4}\left[D\left(x+\frac{\pi}{N}\right) + D\left(x-\frac{\pi}{N}\right)\right]\right\} \qquad \left(D(x) = \frac{\sin\left[\frac{\pi}{T}N\,t_n\right]}{\sin\left[\frac{\pi}{T}t_n\right]}\right)$$

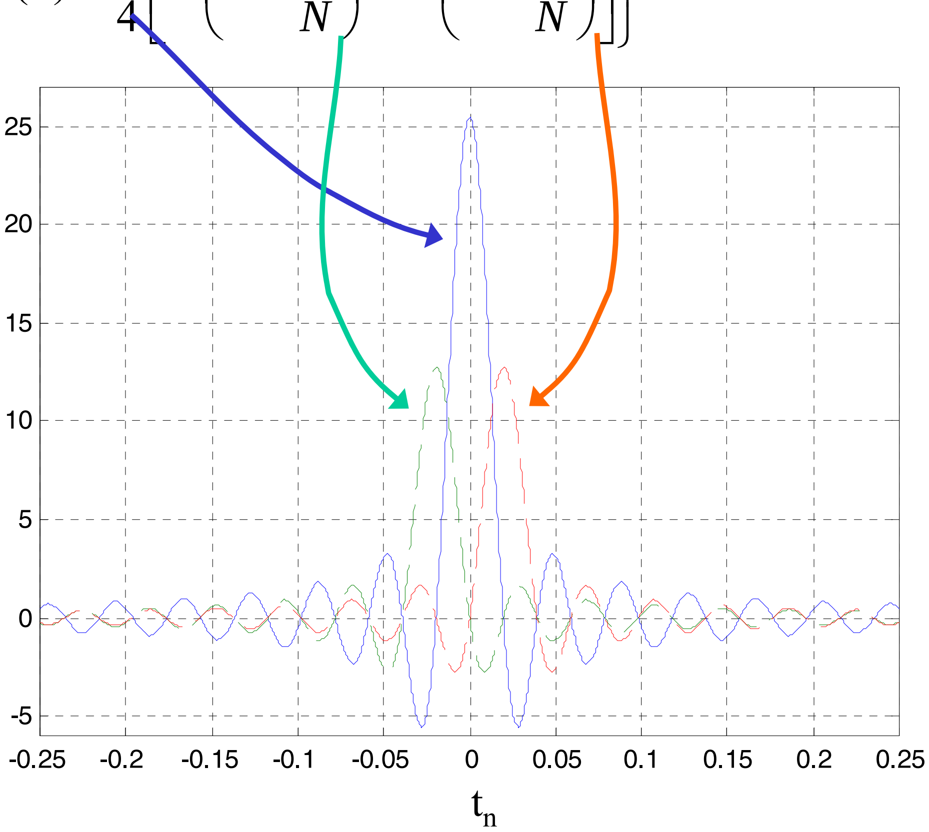

$\cos^{\alpha}(x)$ Windows → Hanning Window (α=2)

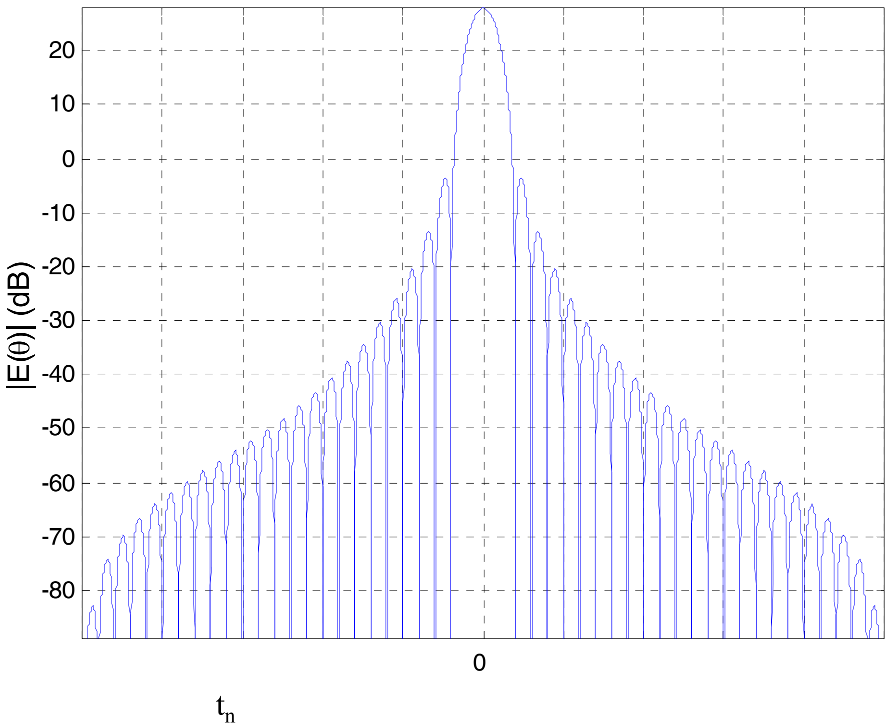

- It does not require extra memory and is controlled by a single parameter.
- Wide enlargement of the main lobe
- Low efficiency: η=0.67
- SLR=32dB
- SL Decay $\propto 1/x^3$ (-18dB/oct) (discontinuity in the second derivative)

Hamming Window (1/2)

The Hamming weights are a modified version of the Hanning weights:

Hanning

$$\begin{cases} w_k = \frac{1}{2} + \frac{1}{2}\cos\left[\frac{2k}{N-1}\pi\right] & k = -\frac{N-1}{2},..,-1,0,1,..,\frac{N-1}{2} \\ g(t_n) = \left\{\frac{1}{2}D(x) + \frac{1}{4}\left[D\left(x+\frac{\pi}{N}\right) + D\left(x-\frac{\pi}{N}\right)\right]\right\} \end{cases}$$

It is obtained by modifying the coefficients of the combination of D(x) functions to achieve a better SL cancellation

$$\begin{cases} w_k = \gamma + (1-\gamma)\cos\left[\frac{2k}{N-1}\pi\right] & k = -\frac{N-1}{2},..,-1,0,1,..,\frac{N-1}{2} \\ g(t_n) = \left\{\gamma D(x) + \frac{1}{2}(1-\gamma)\left[D\left(x+\frac{\pi}{N}\right) + D\left(x-\frac{\pi}{N}\right)\right]\right\} \end{cases}$$

Cancellation of the first sidelobe is for γ=0.543478261. in practice, it is used γ=0.54:

Hamming

$$\begin{cases} w_k = 0.54 + 0.46\cos\left[\frac{2k}{N-1}\pi\right] & k = -\frac{N-1}{2},..,-1,0,1,..,\frac{N-1}{2} \\ g(t_n) = \left\{0.54D(x) + \frac{1}{2}0.46\left[D\left(x+\frac{\pi}{N}\right) + D\left(x-\frac{\pi}{N}\right)\right]\right\} \end{cases}$$

Hamming Window (2/2)

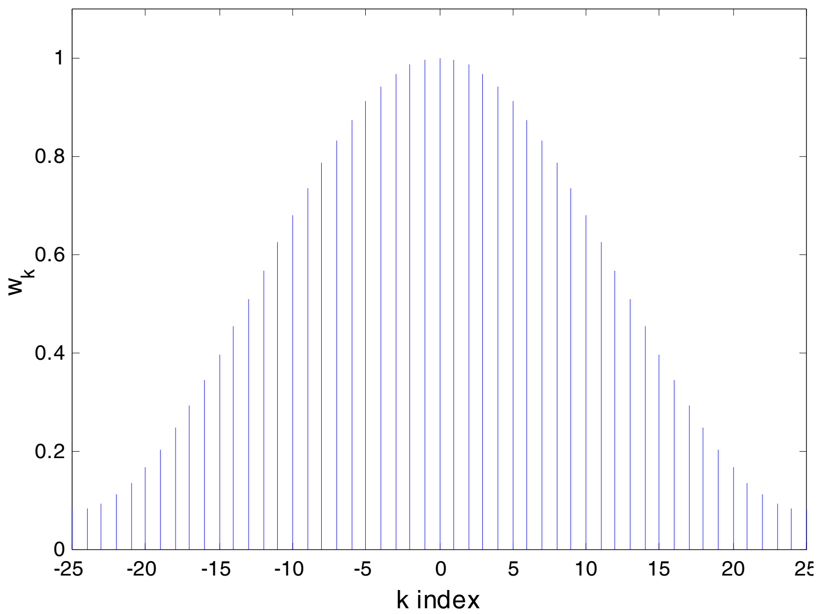

- large attenuation of the first SL of the original compressed waveform
- Better efficiency than Hanning: η=0.73

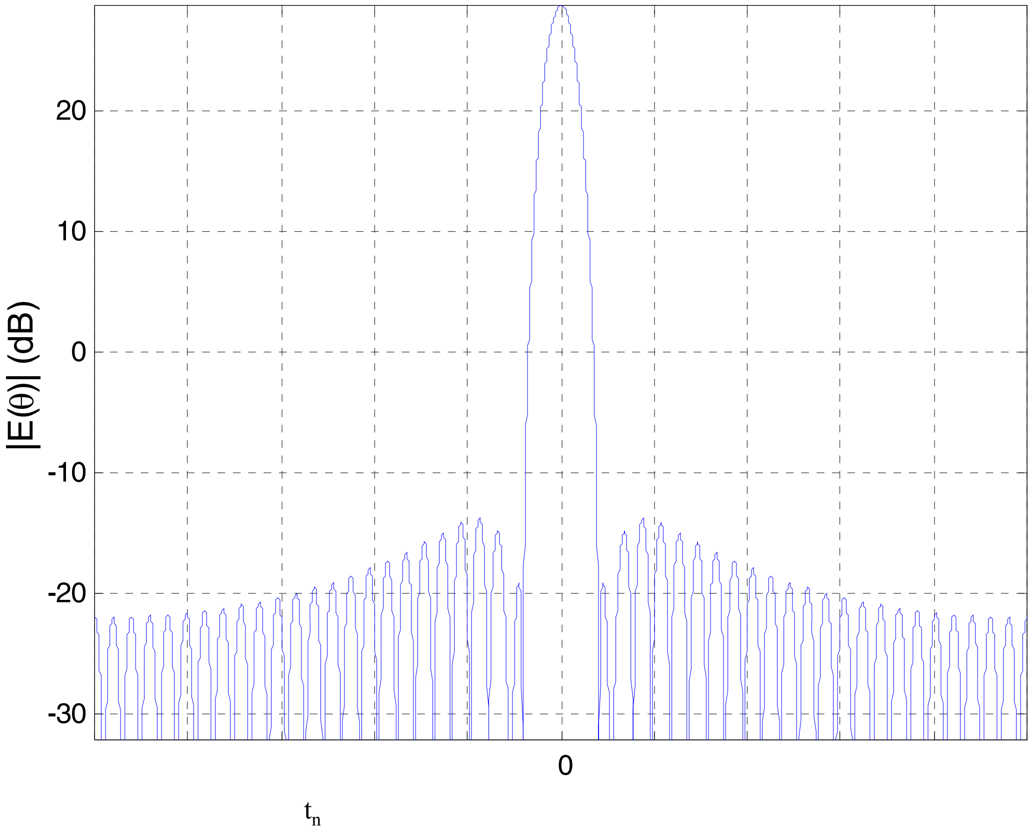

- SLR=43dB
- SL Decay ∝ 1/x (-6dB/oct) (discontinuity at the extremes)

Blackman Windows

- Hanning and Hamming taper functions belong to the "raised cosine" family
- Both are special cases of the Blackman windows (windows function of (N+1)/2 parameters) with only γ_0 and γ_1 non-zero coefficients :

$$w_k = \sum_{m=0}^{(N-1)/2} \gamma_m \cos\left(\frac{2\pi}{N-1} mk\right) \qquad \sum_{m=0}^{(N-1)/2} \gamma_m = 1 \qquad k = -\frac{N-1}{2},..,-1,0,1,..,\frac{N-1}{2}$$

Difficulties with the family of windows:

- The choice of parameters to achieve the desired waveform characteristics is difficult (complex inversion)
- Often the characteristics are not adequate in terms of resolution and efficiency.

Dolph-Chebyshev Window (1/3)

It provides the maximal resolution for assigned sidelobe (costant) level!

The design is based on the properties of the **Chebyshev polynomials** :

$$T_n(u)=\begin{cases}(-1)^n \cosh(n\cosh^{-1}|u|) & u<-1\\ \cos(n\cos^{-1}u) & |u|\le 1\\ \cosh(n\cosh^{-1}u) & u>1\end{cases}$$

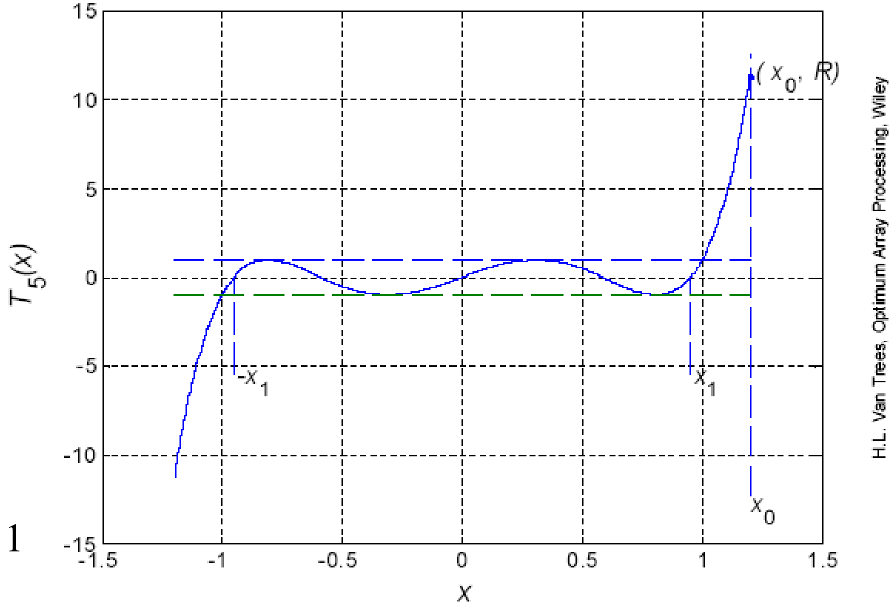

Properties:

- $T_n(u)=2uT_{n-1}(u)-T_{n-2}(u)$
- Zeros in $|u|\le 1$, $u_p=\cos\left[(2p-1)\dfrac{\pi}{2n}\right] \quad p=1,..,n$
- Maxima and minima in $u_k=\cos\left[\dfrac{k\pi}{n}\right] \quad k=1,..,n-1$
- Also $T_n(u_k)=\pm 1$

For a window of N elements, a polynomial with order n=N-1 is used (N-1 zeros).
The oscillating part of the polynomial is used for the sidelobes, while the main lobe is mapped in the region x>1.

Dolph-Chebyshev Window (2/3)

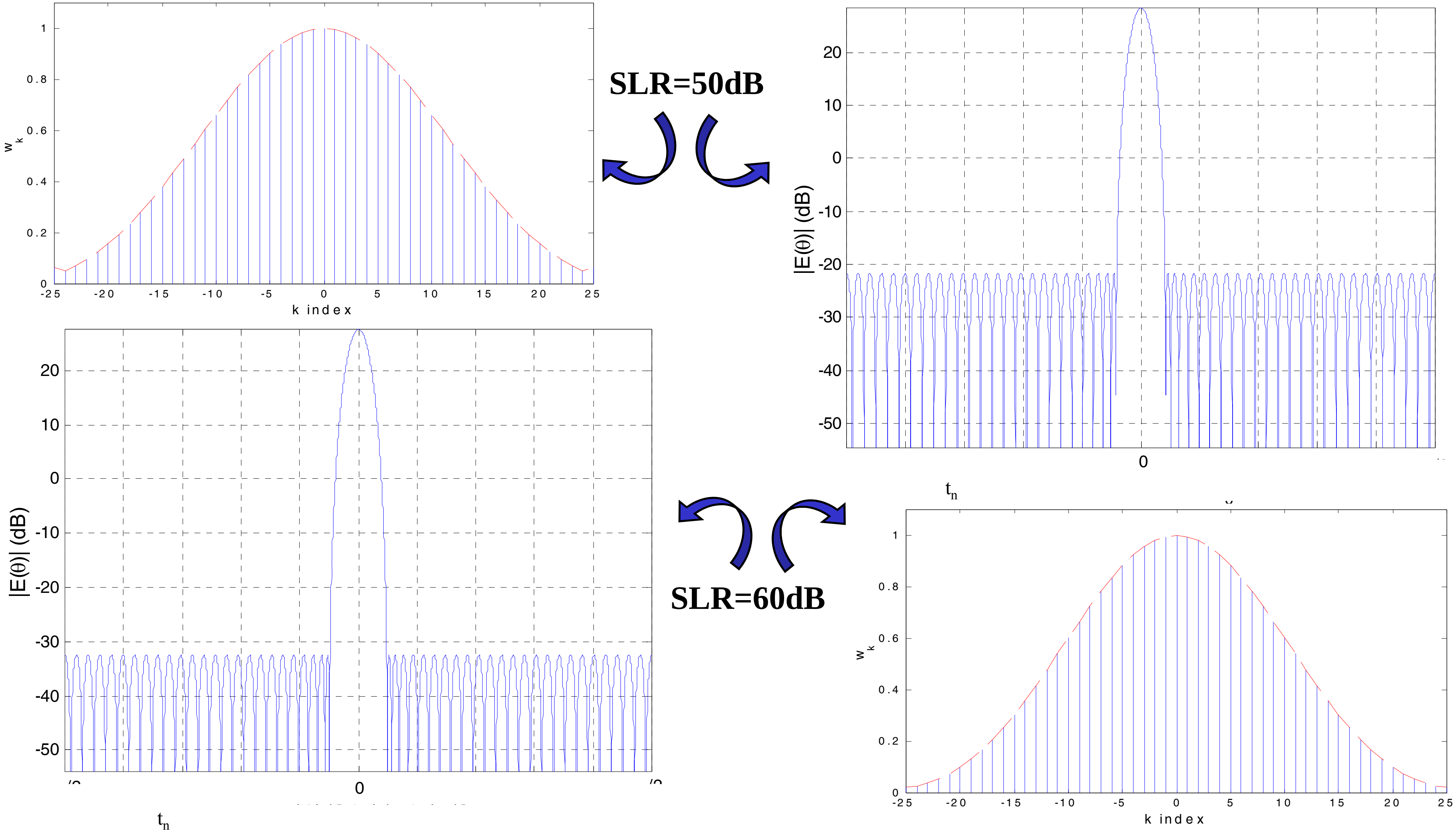

Dolph-Chebyshev Window (3/3)

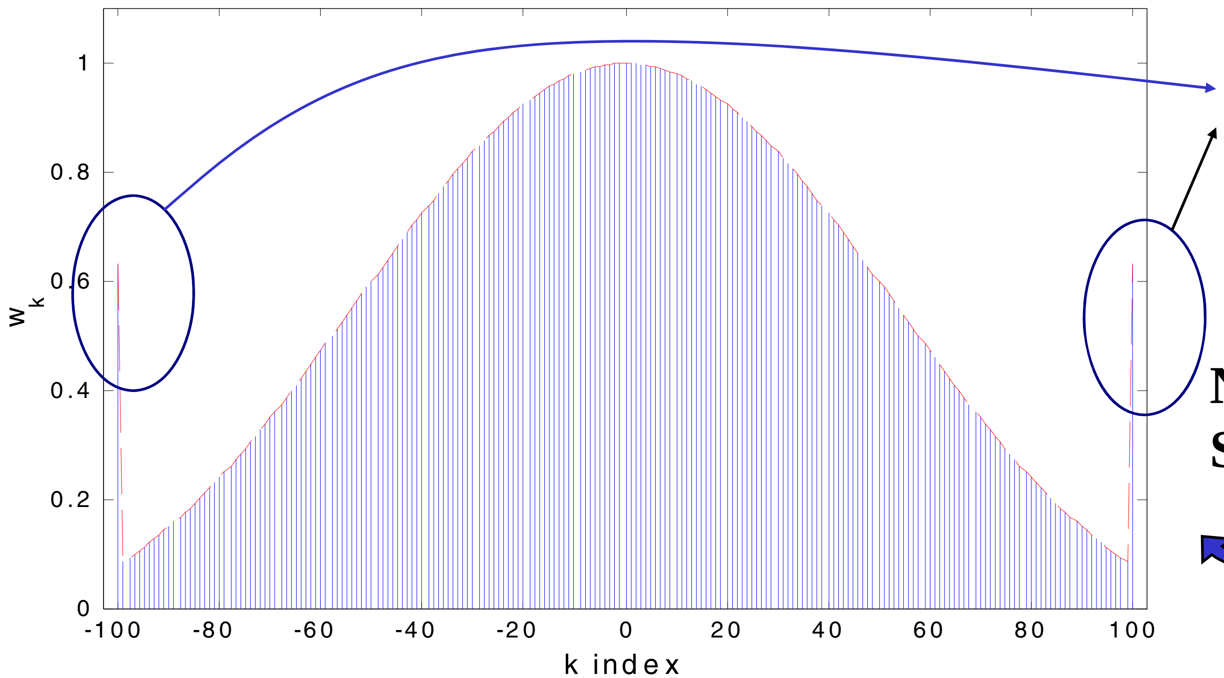

Spike in the taper function!!

N=201
SLR=40dB

For this reason, such taper function is not used in practice.
The Taylor taper function is studied to solve such undesired feature, while keeping the nice properties of the Dolph-Chebyshev solution.

Taylor n-bar Window (1/4)

This is a trade-off between Dolph-Chebyshev taper function with constant RSL and the uniform weights with 1/x sidelobe decay.

Starting point

$$\begin{cases} F(u) = \cosh\left[\pi\sqrt{A^2 - u^2}\right] & u \le A \\ F(u) = \cos\left[\pi\sqrt{u^2 - A^2}\right] & u \ge A \end{cases}$$

- u=2x/π
- Pattern with constant level sidelobes
- There is a transition in the main lobe at u=A between the hyperbolic function and the trigonometric function
- Zeros at → $z_n = \pm\sqrt{A^2 + (n - 1/2)^2}$
- SLR=F(0)=(1/π)coshA

Strategy

Using this ideal pattern, there are still spikes at the window borders → an approximate pattern is used where:

- The first $\bar{n}$ sidelobes are maintained at a constant level
- The pattern zeros are moved to achieve a 1/u behavior in the sidelobe level region far from the main beam

Taylor n-bar Window (2/4)

New zeros:

$$\begin{cases} z_n = \pm\sigma\sqrt{A^2 + (n - 1/2)^2} & 1 \le n \le \bar{n} \\ z_n = \pm n & n \ge \bar{n} \end{cases}$$

$$\sigma = \frac{\bar{n}}{\sqrt{A^2 + (\bar{n} - 1/2)^2}}$$

$$F(u) = \frac{\sin \pi u}{\pi u} \prod_{n=1}^{\bar{n}-1} \frac{1 - \left(\frac{u}{z_n}\right)^2}{1 - \left(\frac{u}{n}\right)^2}$$

Inversion ⇒

$$w_k = \left[1 + 2 \sum_{n=1}^{\bar{n}-1} F(n, A, \bar{n}) \cos\left(n\pi \frac{2k}{(N-1)}\right) \right] / w_{MAX}$$

with $F(n, A, \bar{n}) = \dfrac{[(\bar{n}-1)!]^2}{(\bar{n}-1+n)!(\bar{n}-1-n)!} \prod_{m=1}^{\bar{n}-1} \left[1 - \left(\dfrac{n}{z_m}\right)^2 \right]$

$$k = -\frac{N-1}{2}, .., -1, 0, 1, .., \frac{N-1}{2}$$

Taylor n-bar Window (3/4)

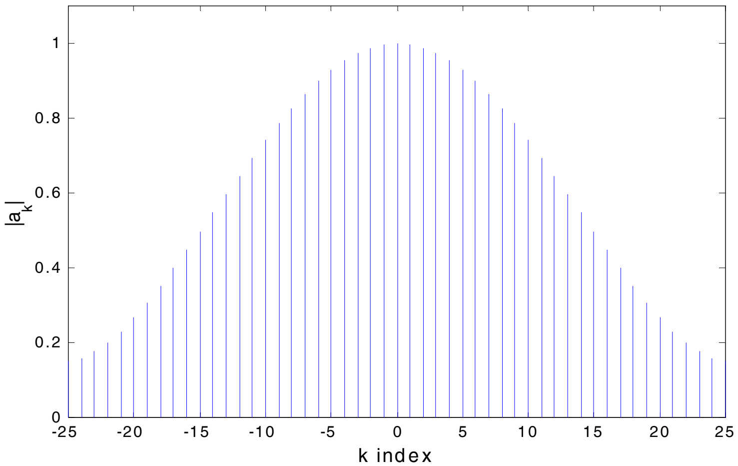

$\bar{n}=5$

SLR=36dB

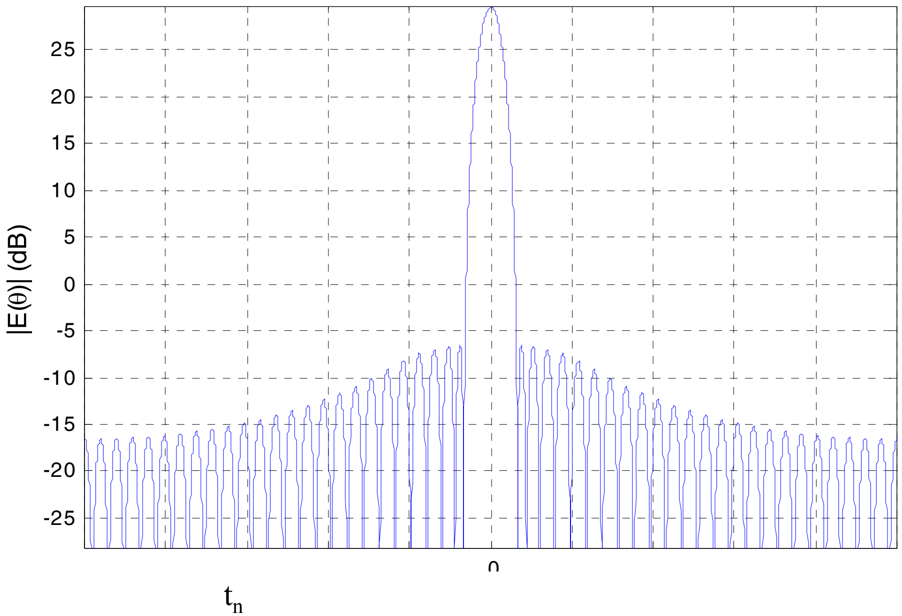

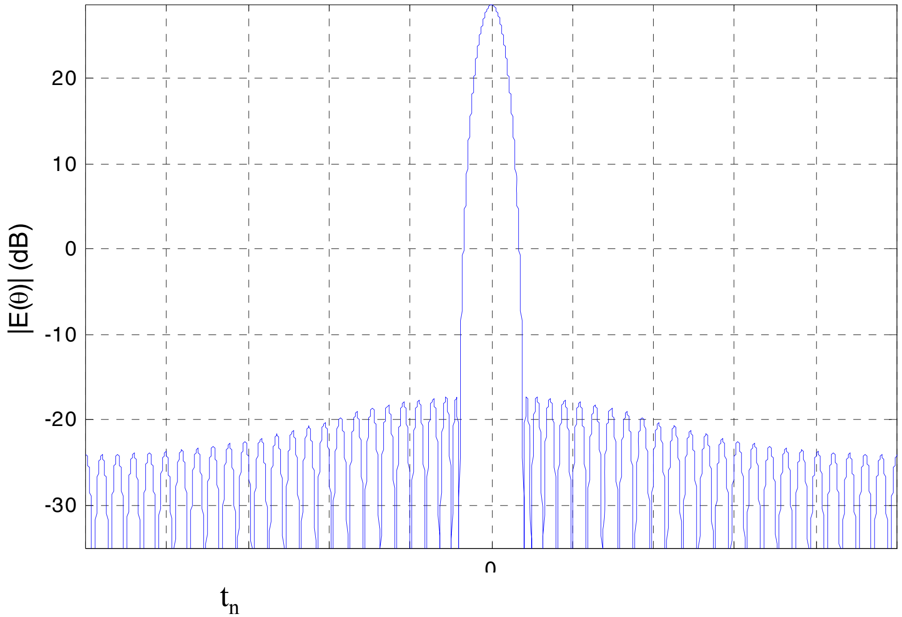

$\bar{n}=8$

SLR=46dB

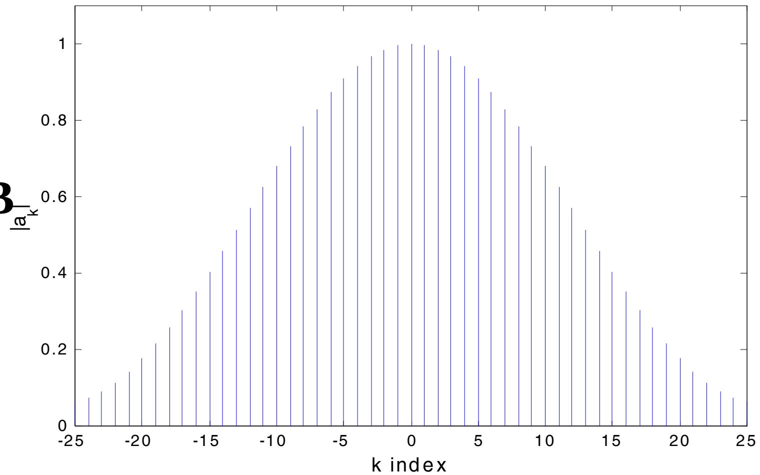

Taylor n-bar Window (4/4)

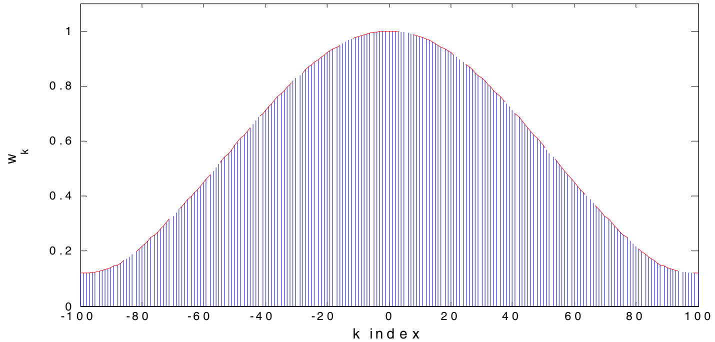

$\bar{n}$ =10

N=201

SLR=40dB

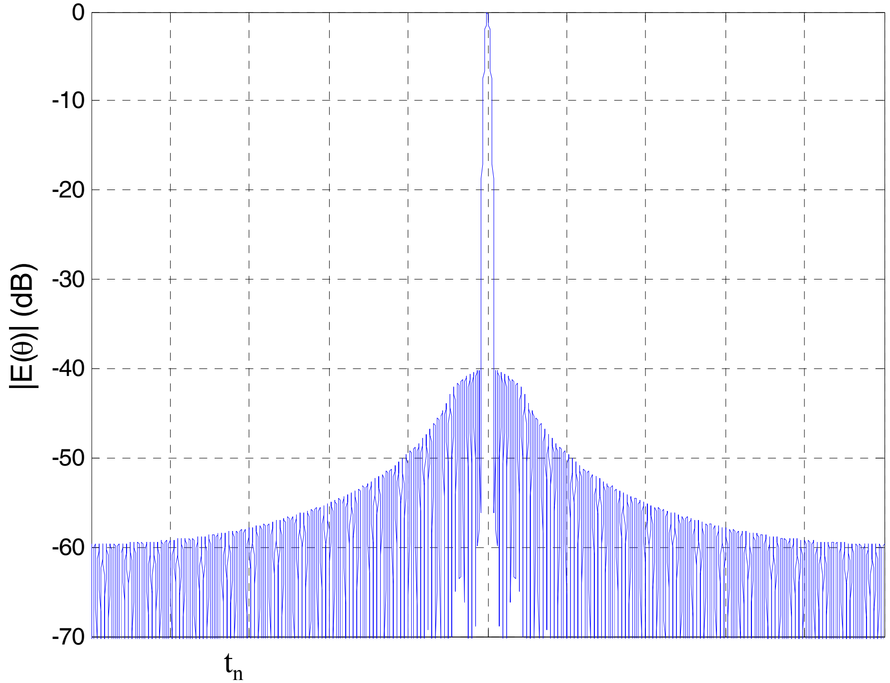

No spikes!

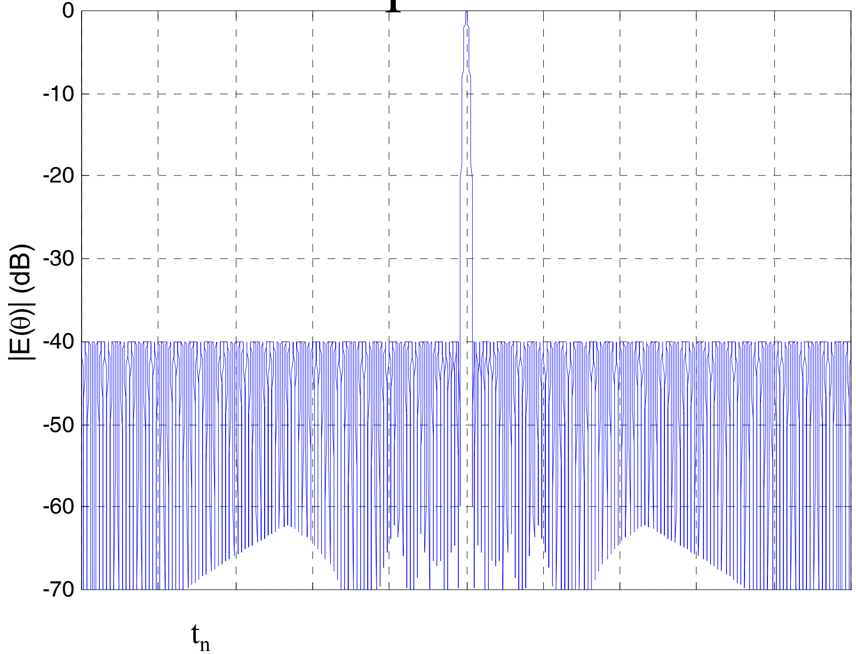

Chebyshev pattern -40dB

- Good approximation for the first SL
- SL asymptotic decay $\propto 1/x$
- Main beam widening
- n cannot be too small for an assigned SLR, but large n values yield implementation problems

Rete di Taylor: coefficienti

4. $w_{Tay}(t) = \sum_{m=-\infty}^{\infty} F_m w_0(t - \frac{m}{B})$

where

$F_0 = 1$, $F_m = 0$ for $|m| \geq \bar{n}$

and

$F_m = F_{-m}$

TAYLOR WEIGHTING:

$W_{Tay}(f) =$

$$W_0(f)\left[1 + 2\sum_{m=1}^{\bar{n}-1} F_m \cos 2\pi m \frac{f}{B}\right]$$

(REFS. 39,42,43)

TABLE 10.9 Taylor Coefficients F_m*

Design sidelobe ratio, dB	−30	−35	−40	−40	−45	−45	−50
$\bar{n}$	4	5	6	8	8	10	10
Main lobe width, −3 dB	1.13/*B*	1.19/*B*	1.25/*B*	1.25/*B*	1.31/*B*	1.31/*B*	1.36/*B*
F_1	0.292656	0.344350	0.389116	0.387560	0.428251	0.426796	0.462719
F_2	−0.157838(−1)	−0.151949(−1)	−0.945245(−2)	−0.954603(−2)	0.208399(−3)	−0.682067(−4)	0.126816(−1)
F_3	0.218104(−2)	0.427831(−2)	0.488172(−2)	0.470359(−2)	0.427022(−2)	0.420099(−2)	0.302744(−2)
F_4		−0.734551(−3)	−0.161019(−2)	−0.135350(−2)	−0.193234(−2)	−0.179997(−2)	−0.178566(−2)
F_5			0.347037(−3)	0.332979(−4)	0.740559(−3)	0.569438(−3)	0.884107(−3)
F_6				0.357716(−3)	−0.198534(−3)	0.380378(−5)	−0.382432(−3)
F_7				−0.290474(−3)	0.339759(−5)	−0.224597(−3)	0.121447(−3)
F_8						0.246265(−3)	−0.417574(−5)
F_9						−0.153486(−3)	−0.249574(−4)

*$F_0 = 1$; $F_{-m} = F_m$; floating decimal notation: −0.945245(−2) = −0.00945245.

Confronto reti di pesatura

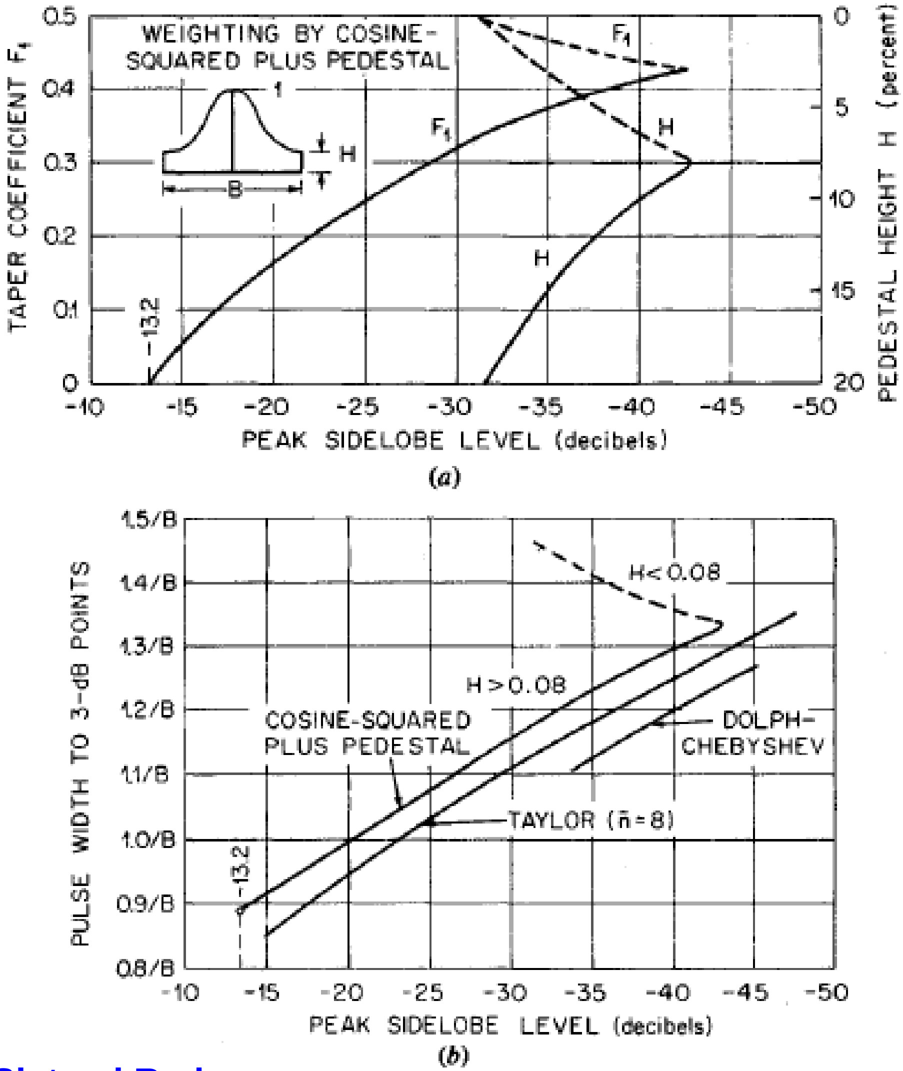

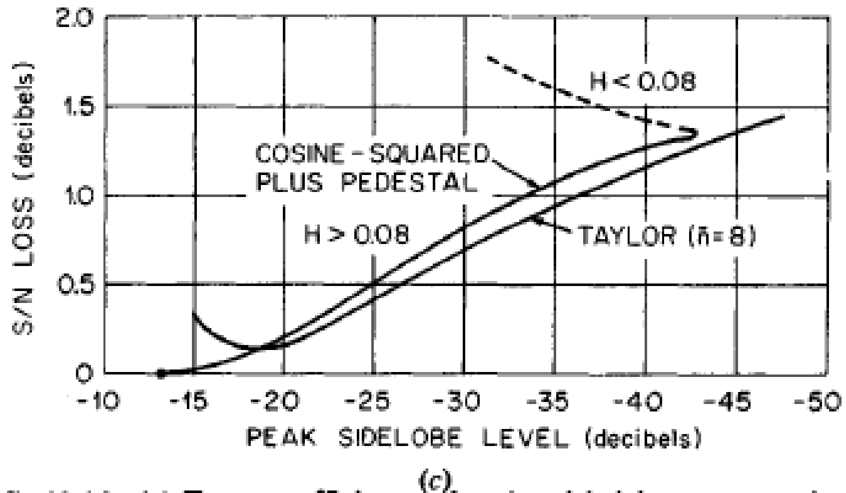

FIG. 10.16 (*a*) Taper coefficient and pedestal height versus peak sidelobe level. (*b*) Compressed-pulse width versus peak sidelobe level. (*c*) *SNR* loss versus peak sidelobe level.

Distorsioni lineari (I)

Effetto delle distorsioni

- Il sistema reale sarà affetto da distorsioni (non sarà esattamente uguale a quello ideale): tutte le distorsioni di sistema possono essere sintetizzate in un filtro distorcente posto in cascata al filtro adattato ideale:

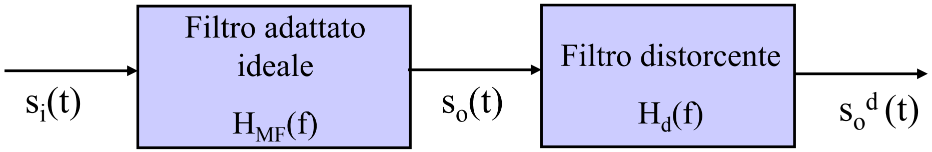

- Nell'ipotesi di piccole distorsioni la $H_d(f)$ può essere sviluppata in serie arrestandosi al primo termine

$$H_d(f) = A(f)e^{jB(f)} \rightarrow \begin{cases} A(f) = 1 + a_1\cos(2\pi C_a f) \\ e^{jB(f)} = e^{jb_1 \sin(2\pi C_b f)} \cong 1 + jb_1 \sin(2\pi C_b f) \end{cases}$$

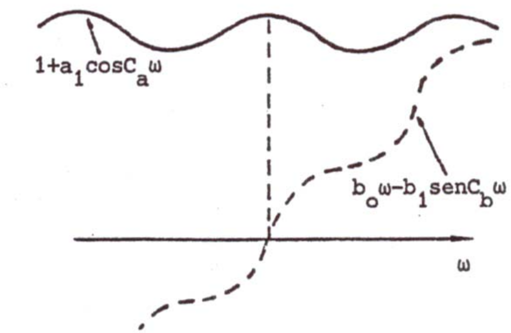

a_1: valore di picco della componente di ampiezza;
b_1: valore di picco della componente di fase;
C_a: frequenza ripple di ampiezza;
C_b: frequenza ripple di fase;

Distorsioni lineari (II)

- Il segnale di uscita distorto è dato da:

$$s_o^d(t) = s_o(t) + \frac{a_1}{2} s_o(t + C_a) + \frac{a_1}{2} s_o(t - C_a)$$ → effetto della distorsione di ampiezza;

$$s_o^d(t) = s_o(t) + \frac{b_1}{2} s_o(t + C_b) - \frac{b_1}{2} s_o(t - C_b)$$ → effetto della distorsione di fase;

ECHI APPAIATI

L'utilizzo di filtri reali anziché ideali comporta la presenza di un disturbo additivo dato dagli echi appaiati: tanto maggiore è a_1&b_1 tanto maggiore è l'ampiezza dell'eco, tanto minore è C_a&C_b (ripple lento) tanto più gli echi appaiati compaiono vicini al segnale utile ⇒ dalle specifiche di dinamica si può ricavare la massima distorsione ammissibile (valore massimo a_1&b_1).

Chirp approximation and sidelobes (II)

- **Side Lobe di Fresnel**

$$S.L.F.\big|_{dB} = 20\,\log(BT) + 3$$

Porzione trascurata nell'approx rettangolare

Importante per bassi rapporti di compressione

Limita la possibilità di abbassare i lobi laterali tramite pesatura

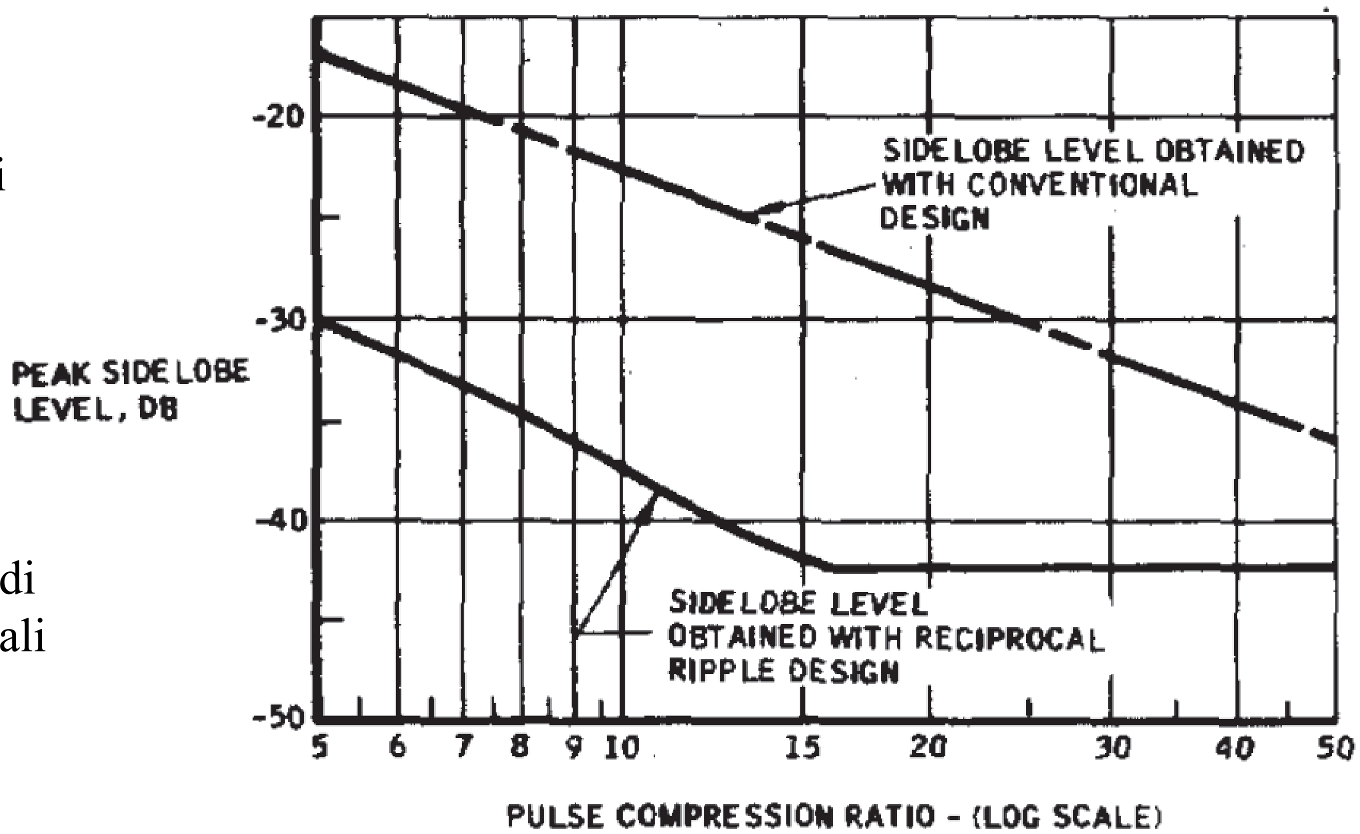

Codici di Barker

Sono codici binari di lunghezza N, caratterizzati da Funzione di AutoCorrelazione (ACF) con lobi laterali in modulo ≤ 1/N

- Esistono solo poche sequenze con queste caratteristiche:

Lunghezza N	**codice**	**PSR (dB)**	**ISLR (dB)**
2	+ -	6,0	3,0
2	++	6,0	3,0
3	++-	9,5	6,5
3	+-+	9,5	6,5
4	++-+	12,0	6,0
4	+++-	12,0	6,0
5	+++-+	14,0	8,0
7	+++--+-	16,9	9,1
11	+++---+--+-	20,8	10,8
13	+++++--++-+-+	22,3	11,5

ACF del codice di Barker da 13

Rispetto ad impulso non modulato τ_p:

- Energia trasmessa BT=n=13 volte superiore
- risoluzione in tempo uguale

- risoluzione in Doppler BT=n=13 volte superiore
- (zona cieca BT=n=13 volte più larga)

Rispetto ad impulso non modulato $T=n\tau_p$:

- Energia trasmessa uguale

- risoluzione in tempo BT=n=13 volte migliore
- risoluzione in Doppler uguale

- (zona cieca uguale)

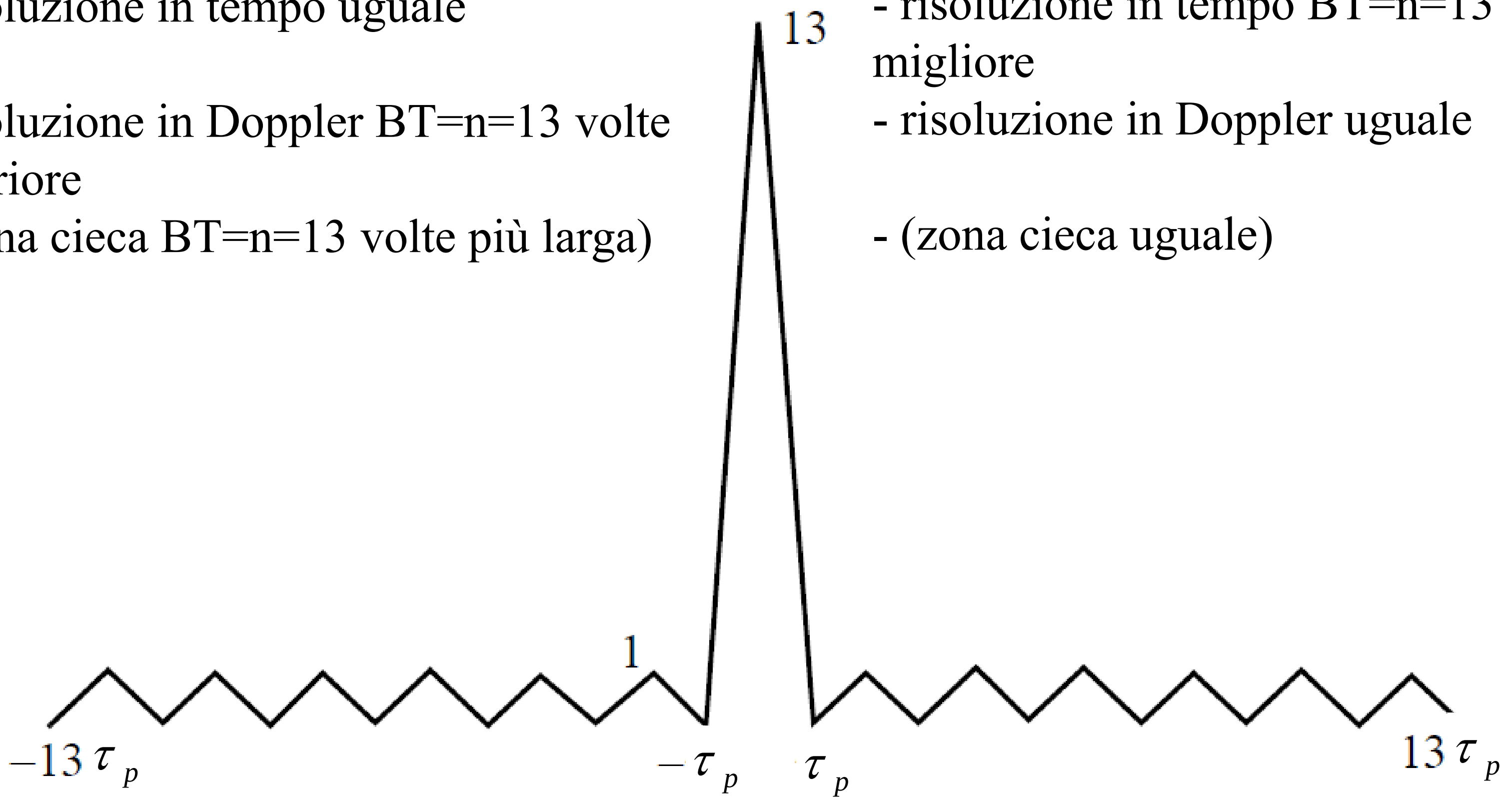

Codice Polifase di Frank (I)

- **Usando M valori di fase**
- **Numero di elementi N=M²**
- **Costruito dalle righe della matrice quadrata:**

$$\phi_{pq} = \frac{2\pi}{M}(p-1)(q-1) \qquad p,q = 1,\cdots,M$$

- **Per N=16**

$$\phi_{pq} \quad \begin{bmatrix} 0 & 0 & 0 & 0 \\ 0 & \pi/2 & \pi & 3\pi/2 \\ 0 & \pi & 2\pi & 3\pi \\ 0 & 3\pi/2 & 3\pi & 9\pi/2 \end{bmatrix} \qquad s_{0\,pq} = e^{j\phi_{pq}} \quad \begin{bmatrix} 1 & 1 & 1 & 1 \\ 1 & j & -1 & -j \\ 1 & -1 & 1 & -1 \\ 1 & -j & -1 & j \end{bmatrix}$$

Codice Polifase di Frank (II)

$$\phi_m = \frac{2\pi}{M}(m-1)\left(\left\lfloor \frac{m}{M} \right\rfloor - 1\right) \qquad m = 1, \cdots, M^2$$

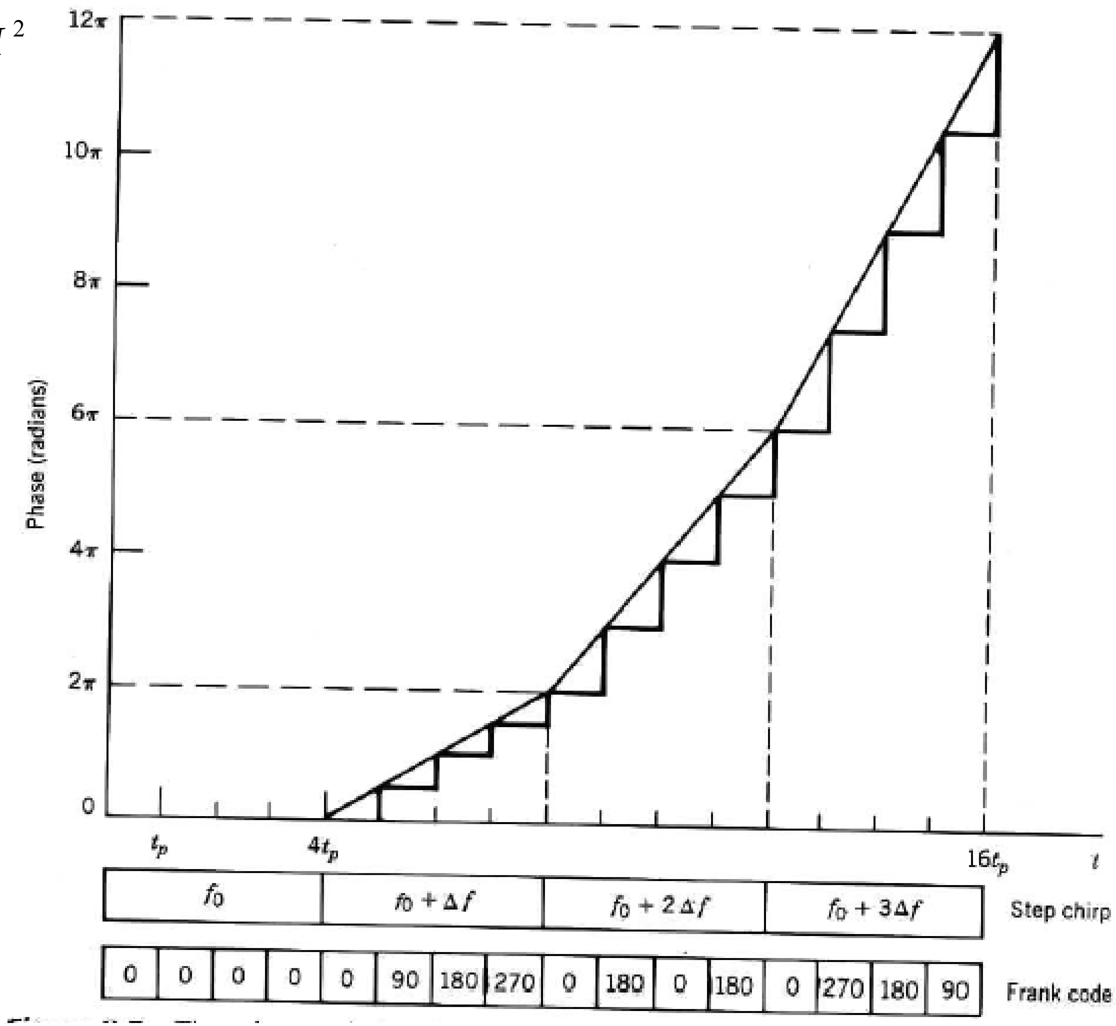

Forma di quantizzazione di un segnale chirp

Codice Polifase di Frank (III)

Table 8.5 The Autocorrelation Sequence of a 16-Bit Frank Code

$\{u_n\}$ / $\{u^*_{N-n+1}\}$	1	1	1	1	1	j	−1	−j	1	−1	1	−1	1	−j	−1	j															
−j	−j	−j	−j	−j	−j	1	j	−1	−j	j	−j	j	−j	−1	j	1															
−1		−1	−1	−1	−1	−1	−j	1	j	−1	1	−1	1	−1	j	1	−j														
j			j	j	j	j	j	−1	−j	1	j	−j	j	−1	j	1	−j	−1													
1				1	1	1	1	1	j	−1	−j	1	−1	1	−1	1	−j	−1	j												
−1					−1	−1	−1	−1	−1	−j	1	j	−1	1	−1	1	−1	j	1	−j											
1						1	1	1	1	1	j	−1	−j	1	−1	1	−1	1	−j	−1	j										
−1							−1	−1	−1	−1	−1	−j	1	j	−1	1	−1	1	−1	j	1	−j									
1								1	1	1	1	1	j	−1	−j	1	−1	1	−1	1	−j	−1	j								
j									j	j	j	j	j	−1	−j	1	j	−j	j	−j	j	1	−j	−1							
−1										−1	−1	−1	−1	−1	−j	1	j	−1	1	−1	1	−1	j	1	−j						
−j											−j	−j	−j	−j	−j	1	j	−1	−j	j	−j	j	−j	−1	j	1					
1												1	1	1	1	1	j	−1	−j	1	−1	1	−1	1	−j	−1	j				
1													1	1	1	1	1	j	−1	−j	1	−1	1	−1	1	−j	−1	j			
1														1	1	1	1	1	j	−1	−j	1	−1	1	−1	1	−j	−1	j		
1															1	1	1	1	1	j	−1	−j	1	−1	1	−1	1	−j	−1	j	
1																1	1	1	1	1	j	−1	−j	1	−1	1	−1	1	−j	−1	j
Output seq.	−j	−1 −j	−1	0	−1	1 +j	j	0	j	−1 +j	1	0	1	1 −j	−j	16	j	1 +j	1	0	1	−1 −j	−j	0	−j	1 −j	−1	0	−1	−1 +j	j

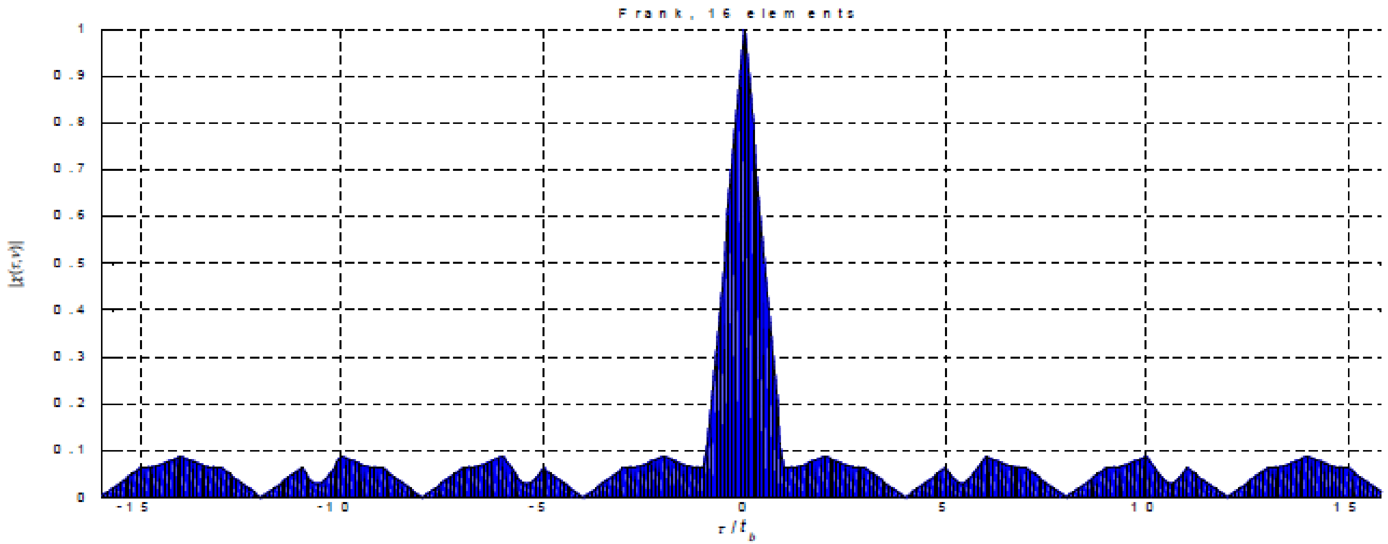

Codice Polifase di Frank (IV)

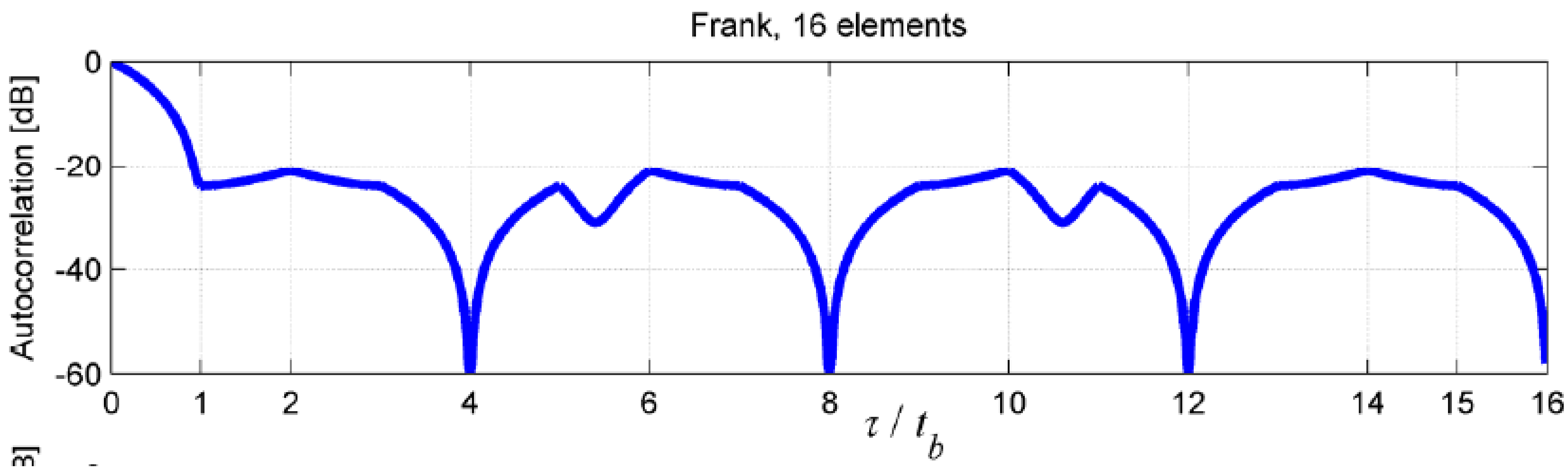

Per N= 16 $\quad PSR = \dfrac{16}{\sqrt{2}} = 8\sqrt{2} = 11{,}3 \quad (21dB)$ *(peggiore di Barker)*

Per N grande $\quad PSR = \pi\sqrt{N} = \pi\ M \quad \Rightarrow 9.94 + 10 * \log_{10}(N)$

(N=100 ~30 dB)

Codici Polifase P3 e P4 (I)

Codice P3

per M pari $\phi_m = \frac{\pi}{M}(m-1)^2 \quad m = 1, \cdots, M$

per M dispari $\phi_m = \frac{\pi}{M}(m-1)\,m \quad m = 1, \cdots, M$

Codice P4

$$\phi_m = \frac{\pi}{M}(m-1)^2 - \pi\,(m-1) \quad m = 1, \cdots, M$$

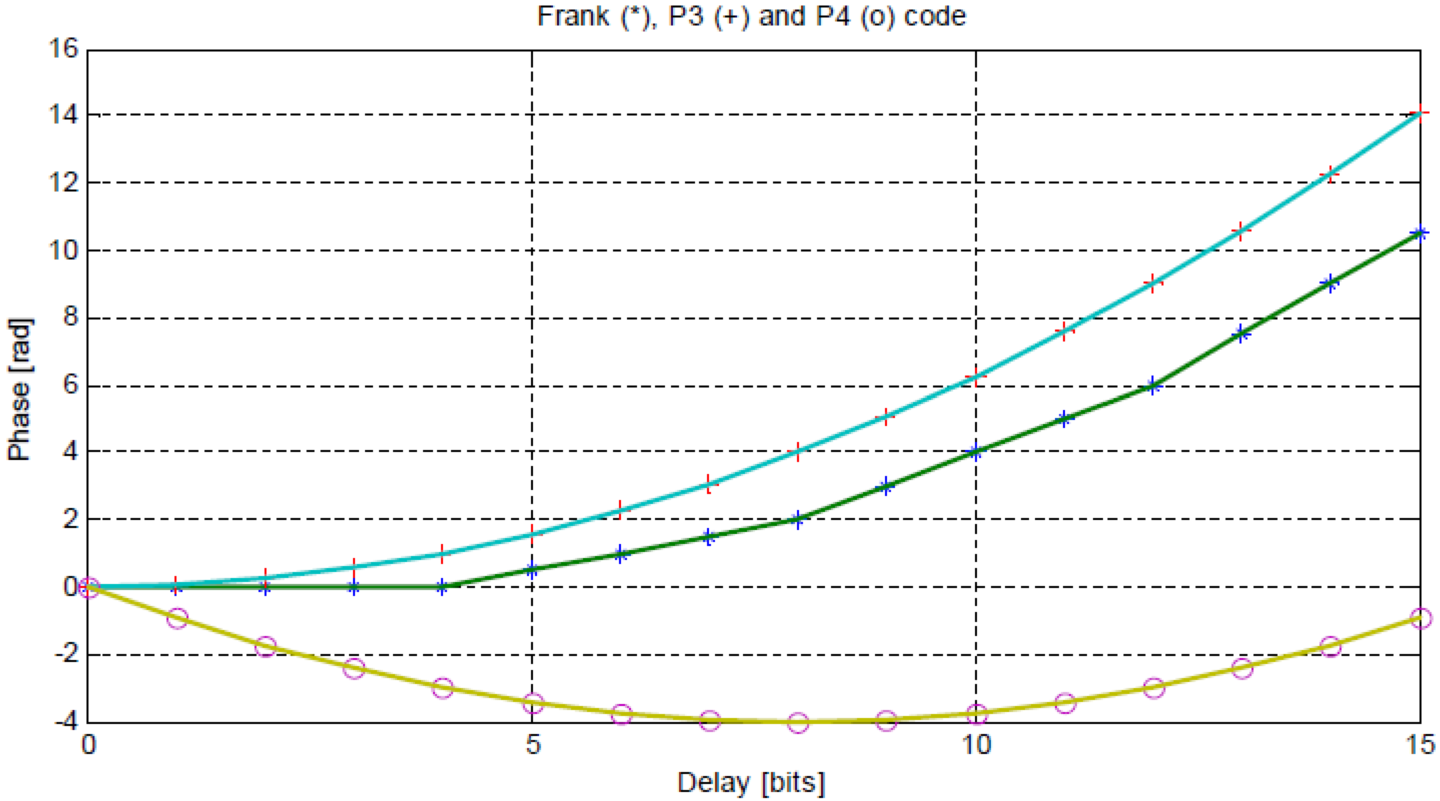

Codici Polifase P3 e P4 (III)